BACHELOR'S THESIS / BIOMEDICAL ENGINEERING 2021

Neuronal basis of brain hypersynchronization in absence seizures: a computational study

Tomas Berjaga Buisan

upf. Universitat Pompeu Fabra Barcelona

Neuronal basis of brain hypersynchronization in absence seizures: a computational study

Tomas Berjaga Buisan

Bachelor's Thesis UPF 2020/2021

Thesis Supervisors:

PhD(c). Pablo Casaní Galdón (Department CEXS)

Prof. Dr. Jordi Garcia-Ojalvo (Department CEXS)

Dedicatory

To my beloved family and friends

Acknowledgments

I consider myself a passionate person who has always been surrounded by numerous people who have helped me in the journey of learning what I have ever wanted. This adventure has not been the less, and I have many people to be grateful for that.

First, the people who I am more thankful for are my supervisors. To Pablo, who has helped me in all the steps of the way, encouraging me to learn a lot of beautiful stuff and making me feel passionate about the subject. I keep excellent memories of the time spent together, either in video calls or in the lab discussing a project I consider from both. Moreover, he has taught me to play chess during our lab breaks, meaning next time we both coincide, I will win.

To Jordi, who has been responsible for all this happening and has allowed me to become a Dynamical Systems Biology lab member for the past months, an absolute honor. Moreover, thanks for the guidance and all your knowledge and experience shared; it means a lot for a student who has always admired you as a researcher.

I also want to thank Pau Clusella and Belén Sancristóbal, who agreed to give me feedback and asses all the work done. It is a pleasure being in touch and receive comments from two great computational neuroscientists.

I also want to acknowledge all the Dynamical Systems Biology lab members for fruitful and enjoyable conversations.

Furthermore, I also want to thank all my Hormonic teammates and friends (Miriam, Quim, Edu, Andreu, and Jaume) for all the talks about our bachelor's thesis, ideas, breaks, and support during the journey.

Also, thanks to my dear friend Imene, who helped me in correcting the thesis written part.

I want to especially thank all my family and friends for the unconditional support along this adventure, as in all the other projects and decisions I have taken in my life.

I want to finish by thanking whoever is reading this thesis for dedicating his time to reading and enjoying all that I have been working on the past year. Thanks!

Abstract

Absence seizures are generalized epileptic seizures mainly diagnosed and prevalent in children and are caused by abnormal electrical brain activity. These seizures initiate in layer 5/6 of the primary somatosensory cortex and are associated with genetic-based channelopathies. More than thirty mutations in genes encoding T-type calcium channels, with a gain-of-function profile, have been linked to absence epilepsy. These channels are the actual front-line treatment target and have been identified in the axon initial segment (AIS) of the above-mentioned primary somatosensory layer 5 pyramidal cells, a domain that plays a major role in neuronal excitability. AIS T-type calcium channels are crucial for bursting, so that any perturbation could potentially lead to epileptogenesis through increased synchronicity. This thesis aims to understand how T-type calcium channels located in the AIS of neurons lead to bursting and how such bursting affects brain oscillations and their synchronization in the somatosensory cortex network. We have designed and implemented a computational model that will enable us to understand the basic neural mechanisms underlying hypersynchronization states in the initiation foci of absence epileptic seizures. To do that, we describe mathematically somatosensory pyramidal neurons with a compartmentalized integrate-and-fire model, extended to include AIS T-type calcium channels. We also connect these neurons to the two main cortical interneuron populations via conductance-based synapses. Our results show that an upregulation of the T-type calcium channel leads to an increase in synchronized activity in local cortical networks in different oscillatory regimes, explaining how these channels could be responsible for hypersynchrony and seizure initiation.

Keywords

Brain, Epilepsy, Absence Seizures, Hypersynchronization, Pyramidal Neuron, Somatosensory Cortex, Bursts, Axon Initial Segment, T-type Calcium Channel, Integrate-and-Fire.

Prologue

> " Finite entities will never be able to understand the infinity surrounding us. Despite this true and disappointing fact, if a single answer could help people, all efforts to tackle it will be worthwhile. "
>
> Tomás Berjaga González - My father

Brain research is constantly evolving to understand and treat some of the pathologies affecting millions of people worldwide. Despite brain data is growing exponentially, our knowledge about brain mechanisms and disorders is increasing in a sublinear manner [1]. Therefore, to solve such complexity, we must build something to understand it, as stated by Richard Feynman. For that, computational neuroscience represents a valuable approach as it enables us to give insight into dynamics challenging to measure in vivo by describing the brain with computation and mathematics. The importance of the field is such that Alan Hodgkin and Andrew Huxley won in 1952 the Nobel prize, the only one in the mathematical modelling field, for their mathematical model that was able to describe the neuron action potential initiation and propagation.

To be able to model different neuronal mechanisms and processes, it must be considered that the brain operates at different temporal and spatial scales. In fact, information is processed in milliseconds by neurons, integrated into brain networks in seconds, stored in memories in days, and defining our behavior for decades. Then, to determine what is happening at different scales, we must first figure out what happens in the fundamental brain unit, the neuron.

This thesis aims to understand the underlying mechanisms in neurons for the most common neurological disease, epilepsy. In other words, the main objective is to give insight into the resulting brain hypersynchronization states in absence seizures, mainly affecting school-age children, by using neuronal mathematical models. This work represents a further step into the final comprehension of the relation between genetic-based channelopathies, network hypersynchrony, seizure initiation at the foci, and the absence generalized epilepsies.

Index

1 Introduction **1**
1.1 Epilepsy and Absence Seizures . . . 1
1.2 Spike and Burst Initiation Area: The Axon Initial Segment . . . 2
1.3 Transient Low-Voltage-Activated Calcium Channels . . . 3
1.4 Thesis Hypothesis and Objectives . . . 5

2 Methods **6**
2.1 Neuronal Injection Inputs . . . 6
2.1.1 Ornstein-Uhlenbeck Stochastic Process . . . 6
2.1.2 Oscillatory Poisson Process . . . 6
2.2 Single-cell and Ionic Channel Models . . . 7
2.2.1 Layer 5 Somatosensory Cortex Pyramidal Model . . . 7
2.2.2 The AIS T-type Calcium Channel Model . . . 10
2.2.3 Parvalbumin Fast-Spiking Interneuron . . . 12
2.2.4 Somatostatin Low-Threshold Spiking Interneuron . . . 13
2.3 Primary Somatosensory Cortex Network . . . 15
2.3.1 Network Connectivity . . . 16
2.4 Network Analysis . . . 17
2.4.1 Spike and Bursting Metrics . . . 17
2.4.2 Spectral Analysis . . . 17
2.5 Technical Information . . . 18

3 Results **19**
3.1 AIS T-type Calcium Channels Trigger Burst Firing . . . 19
3.2 AIS T-type Calcium Channels Promote Primary Somatosensory Layer 5 Synchronicity . . . 20
3.2.1 Pyramidal Network . . . 20
3.2.2 SOM-dominating Network . . . 22
3.2.3 PV-dominating Network . . . 23
3.2.4 Symmetrically Coupled Network . . . 25

4 Discussion **26**
4.1 Conclusion and Future Perspectives . . . 28

Bibliography **29**

Supplementary information **37**
S.I Ornstein-Uhlenbeck Derivation by Itô's Calculus . . . 37
S.II Model Parameters . . . 39
S.II.1 Layer 5 Somatosensory Cortex Pyramidal Model . . . 39
S.II.2 The AIS T-type Calcium Channel Model . . . 39
S.III Additional Results . . . 40
S.III.1 SOM-dominating Network . . . 40
S.III.2 PV-dominating Network . . . 40
S.III.3 Symmetrically Coupled Network . . . 41

List of Figures

1 Location of the Axon Initial Segment in a Motoneuron Cell 3
2 Cav3 Structure 4
3 Oscillatory Poisson Process Input Generation 7
4 Response of the Layer 5 Pyramidal Somatosensory Neuron to an AIS and Somatic Injection 8
5 Response of the Layer 5 Pyramidal Somatosensory Neuron to a Dendritic Injection 9
6 Layer 5 Pyramidal Somatosensory Neuron Frequency with Respect to Input 10
7 AIS T-type Calcium Channel Activation and Inactivation Gating Variables and Maximal Injected Current 11
8 AIS T-type Calcium Channel Activation Time Constant 12
9 AIS T-type Calcium Channel Inactivation Kinetics 12
10 PV-expressing Interneuron Response 13
11 PV-expressing Interneuron Firing Frequency with Respect to Square-Pulse Injections 13
12 SOM-expressing Interneuron Response 14
13 SOM-expressing Interneuron Firing Frequency with Respect to Square-Pulse Injections 15
14 Primary Somatosensory Cortex Layer 5 Network Schematics and Dynamics 15
15 AIS T-type Calcium Channel Effect on Firing Behaviour 19
16 AIS T-type Calcium Channel Effect on Firing Behaviour 20
17 Pyramidal Network Multitaper Power Spectrum for Different AIS T-type Calcium Conductances. 20
18 Pyramidal Network Burst Events for Different AIS T-type Calcium Conductances. 21
19 Pyramidal Network Time-Frequency Plots 21
20 SOM-dominating Network Multitaper Power Spectrum for Different AIS T-type Calcium Conductances. 22
21 SOM-dominating Network Burst Events for Different AIS T-type Calcium Conductances. 22
22 SOM-dominating Network Time-Frequency Plots 23
23 PV-dominating Network Multitaper Power Spectrum for Different AIS T-type Calcium Conductances. 23
24 PV-dominating Network Burst Events for Different AIS T-type Calcium Conductances. 24
25 PV-dominating Network Time-Frequency Plots 24
26 Symmetrically Coupled Network Multitaper Power Spectrum for Different AIS T-type Calcium Conductances. 25
S1 SOM-dominating Network Multitaper Power Spectrum for Different Injected Currents and AIS T-type Calcium Conductances. 40
S2 PV-dominating Network Multitaper Power Spectrum for Different AIS T-type Calcium Conductances. 41
S3 Symmetrically Coupled Network Multitaper Power Spectrum for Different AIS T-type Calcium Conductances. 41
S4 Symmetrically Coupled Network Burst Events for Different AIS T-type Calcium Conductances. 42

S5 Symmetrically Coupled Time-Frequency Plots 42

List of Tables

1 SOM-dominating and PV-dominating Network Connectivity Matrix 17
2 Symmetrically Coupled and Pyramidal Network Connectivity Matrix . . . 17
S1 Layer 5 Somatosensory Cortex Pyramidal Model Parameters 39
S2 AIS T-type Calcium Channel Model Parameters 39

1 Introduction

1.1 Epilepsy and Absence Seizures

Epilepsy is the most common, chronic, severe neurological disease, affecting more than 65 million people worldwide [2]. It is mainly characterized by recurrent abnormal neuronal hypersynchronization, also known as seizures, that could potentially lead to disabilities, other disorders, and death [3, 4]. Idiopathic generalized epilepsies (IGE) are genetic-related channelopathy disorders and represent one-third of all epilepsies [5]. Childhood absence epilepsy (CAE), a type of IGE, is the most common paediatric epileptic syndrome, and it is distinguished by the appearance of absence seizures [6, 7]. These seizures have a frequency from a few to a hundred per day and are characterized by brief, sudden and uncontrolled loss of consciousness [8, 9]. Therefore, patients exhibiting this illness can have many physiological and psychological problems in their daily life.

During ictal electroencephalogram (EEG) recordings, absence seizures show a rhythmic and synchronous bilateral pattern of 3 Hz spike-and-wave discharges (SWD) [7, 8, 10]. The appearance of SWD could be resulting from the alteration of the feedback interactions between the somatosensory cortex (SoCx) and the thalamus [8, 11, 12, 13]. Moreover, different clinical studies prove an augment in the EEG background activity, beta and gamma rhythms, during interictal and ictal periods that could be resulting from hyperexcitability in local networks [7, 13].

Recent experimental data from animal models show that the initiation foci of absence seizures are the deep layers (layer 5/6) of the primary SoCx. Once initiated, it interacts with the thalamus that acts as a resonant circuit, thus, disrupting the whole oscillatory pattern [7, 10]. In a more detailed way, multiple studies have demonstrated and showed the hypersynchronous primary SoCx layer 5 epilepsy foci in two different rat genetic models of absence epilepsy: the Wistar Albino Glaxo/Rijswijk (WAG/Rij) and the Genetic Absence Epilepsy Rats from Strasbourg (GAERS) [5, 6, 14, 15]. In addition, the foci and their local networks show increased intrinsic excitability, synchronization, and elevated spontaneous firing rate during ictal periods [5].

Intracellular calcium increases during the ictal period, relating calcium channels to seizure initiation and propagation [16]. In fact, multiple human clinical studies have linked more than 30 genetic upregulations of the transient low-voltage-activated (T-type) calcium channels to absence seizure initiation, suggesting it as the primary pathogenic event [17, 18, 19, 20, 21]. An increase in T-type currents and genetic variations with upregulation profiles have also been observed in the above-mentioned rats and mice absence seizure models [22, 23]. Furthermore, experimental studies also show that T-type calcium channel deficient mice are resistant to external absence seizure genesis [8]. Additionally, it is known that T-type calcium channels promote network synchronization by generating burst-firing behaviour in the network, which is an absence seizure hallmark [17, 21].

These channels are the actual front-line treatment target as the main prescribed drug for absence epilepsy is ethosuximide, a T-type calcium channel blocker [8, 9, 20]. Moreover, three other blockers have been approved for clinical use in absence seizures [24]. These drugs decrease T-type calcium currents, thus, stopping the seizure [24]. Despite this fact, ethosuximide is not only targeting T-type calcium channels as it is additionally

partially blocking sodium and calcium-dependent potassium channels [21, 24]. The broad tissue expression of the channel has also complicated clinical drug development as it has been challenging to target the channels in the neuronal excitability focus [24]. Therefore, pharmacological research goes in the direction of finding more specific targeting drugs for eliminating drug side effects and for treating non-treatment responding absence seizures [3, 4, 17]. Hence, for tackling a complex multi-nodal disease like epilepsy, it is critical to understand how T-type calcium channels, especially those located at the spike generation foci, affect the bursting mechanisms and local SoCx network neurotransmission. Then, the study of how T-type calcium channels elevate neurotransmission and information transfer in seizures could give us an insight into absence seizure trigger mechanisms to find targets to develop future potential therapeutics.

1.2 Spike and Burst Initiation Area: The Axon Initial Segment

Neuronal cells encode and transfer information with action potential (AP) emission, also referred to as spikes, which are generated due to membrane depolarizations once the neuron overpass a certain threshold [25, 26]. Spikes can be emitted in a tonic form or emitted in periods of high-frequency spiking, also known as burst firing [27, 28]. This last mechanism turns out to be vital in encoding neuronal information and in pathologies with elevated neurotransmission [28]. Being able to discern and understand spiking and bursting generation and propagation could help us understand brain information transmission and the mechanisms underlying disorders as the above-mentioned epilepsy.

The axon initial segment (AIS) is the responsible for AP initiation in mammalian neuronal cells [29, 30]. The first pieces of evidence suggesting the AIS role were found in motoneurons back in the 1950s by Coombs and co-workers [31]. Recently, more neuronal subtypes have been demonstrated to have the AIS as the spike generation focus, including hippocampal, pyramidal primary SoCx layer 5, or cartwheel cells [29, 32, 33]. In SoCx layer 5 pyramidal neurons, voltage-sensitive dyes indicate that the AP is generated in the distal region of the AIS domain without the action of Ranvier nodes [29].

AIS is an unmyelinated axonal 20-60 μm region located at the proximal axon/soma interference, and it starts just after the axon hillock (See Fig. 1) [33, 34]. It is mainly characterized by the high density of voltage-gated channels that are clustered in ankyrin-G master scaffolding, which is also responsible for neuronal polarity [34, 35]. Antibody staining techniques indicate a higher Na+ channels density in comparison with proximal dendrites and soma compartments, thus, allowing the region to have a lower potential for spike initiation [36]. Little is known about differences in gating variables, which could also play a crucial role [34]. Moreover, there is an order of magnitude decrease in diameter from soma to AIS, together with a reduction in capacitance, allowing the AIS to be energetically favourable as it requires less inward current for AP initiation [33]. This and the advantage of having only an initiation spot for AP inhibition could explain the reason why evolution has selected the AIS domain in vertebrates [33].

Diversity in AIS composition, geometry, location and other properties among different subtypes could be responsible for different neuronal outputs in response to synaptic inputs, thus explaining different neuronal dynamical behaviours [33, 37].

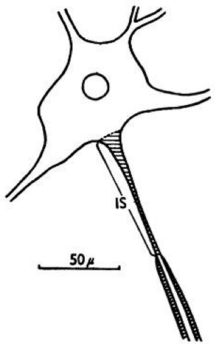

Figure 1: Location of the axon initial segment (Labeled as IS) in a motoneuron cell. Adapted from Coombs and co-workers [31].

Furthermore, they are characterized for having T-type calcium channels, which are responsible for controlling bursting by generating low-voltage calcium spikes [34]. Then, it is fair to say that AIS positioning and properties allow the domain to modulate neuronal excitability perfectly. Hence, as small perturbations could generate significant differences in excitability and spike generation, it is not surprising that the AIS is related to many neurological pathologies [33, 35]. In fact, hundreds of mutations in ion channels are known to be associated with epileptogenesis, especially those affecting low-threshold calcium spikes [19]. Essential aspects of how ionic channel mutations affect the spiking dynamics and the local networks remain unclear. Another critical aspect that is unclear and could play a predominant role in AIS functioning are the GABA-mediated synapses that innervate and target the domain, representing the unique exclusive input in the AIS of cortical pyramidal neurons [30, 33]. All this could represent a considerable change in a network environment as effects on the APs, and in consequence in neurotransmitter release and synaptic input, could immensely impact oscillatory behaviours and synchronicity.

In summary, the AIS dynamics and perturbations study is vital for understanding the mechanisms for information transfer and pathologies as it represents an essential regulator for neuronal firing patterns. Then, the study of the T-type calcium channels and their effects on spiking and bursting activity is critical to underlie the neurotransmission alterations in pathogenic states.

1.3 Transient Low-Voltage-Activated Calcium Channels

The appearance of low-threshold calcium spikes (LTS) that trigger the spike was first recorded in 1978 by Moolenad and Spector [38]. Its existence in neuronal cells is due to the existence of low-voltage-activated (LVA) calcium channels that facilitate the cell to reach the AP threshold by depolarizing typically 25 mV [39, 40]. Multiple experimental studies concluded that LTS were mediated by a transient calcium channel called transient LVA (T-type) calcium channel [39, 41]. Even though the structure is not well resolved, T-type calcium channels are exclusively formed by the main Cav3 pore-forming unit, a peculiarity among other ion channels (See Fig. 2) [24, 42]. There are three different subtypes of Cav3, encoded by *CACNA1G*, *CACNA1H*, and *CACNA1I*, located on chromosomes 17, 16, and 22, respectively, forming three-channel isoforms Cav3.1, Cav3.2, and Cav3.3 [43, 44, 45].

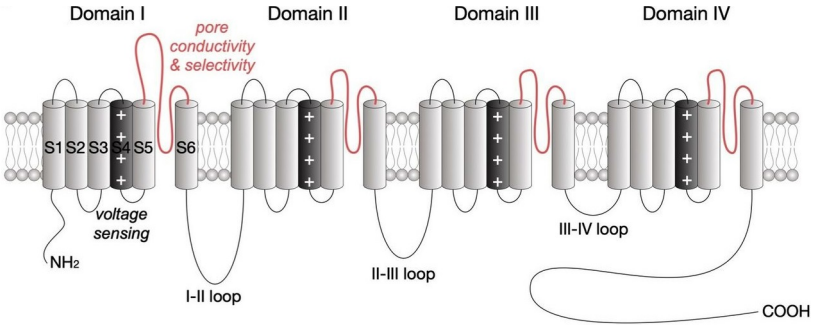

Figure 2: The Cav3 subunit structure. It is a 260 kDa protein organised into four hydrophobic domains (DI to DIV), each of them made of six transmembrane helices (S1 to S6). From Weiss et al. (2020) [24].

These channels are widely distributed along the neuron and are characterized for activating near the resting membrane potential, thus having only a small range where Cav3 can be open, but without being completely inactivated [39, 46, 47, 48]. They open at a relatively hyperpolarized membrane potential, -70 to -50 mV, lower than sodium channels threshold, and in consequence, being able to influence whether and how a neuron will emit an AP [21, 24, 49]. Cav3.1 and Cav3.2 isoforms open and close at approximately similar membrane potentials, but Cav3.3 opens at more depolarized potentials (Similar to what happens during channel inactivation) [50]. The kinetics are behaving differently also in the isoforms (Faster Cav3.1 $>$ Cav3.2 $>$ Cav3.3 slower) [21, 39, 51]. Their effect on neuronal excitability is due to their presence in the AIS of multiple neuronal types, including in the primary SoCx layer 5 pyramidal neurons, cartwheel cells, and Purkinje cells [52]. In fact, due to their characteristics and positioning in the AIS, T-type calcium channels have been seen to trigger rebound burst firing in different populations [52, 53, 54, 55].

Considering multiple animal and human studies and the essential role of T-type calcium channels in neuronal excitability, it is not surprising that alterations in their function relate to multiple neurological disorders such as Parkinson, pain perception, or the mentioned absence seizures [18, 56, 57, 58].

It is thought that in absence seizures, as explained before, an increase in channel expression and performance alter burst patterns by increasing the number of them. In turn, an increase in burst firing is supposed to increase the synchronicity of oscillations, as a burst releases a more significant amount of neurotransmitter, thus allowing the postsynaptic cell not to filter the signal and burst as the previous. In other words, increased neurotransmission increase synchronicity and triggers the absence seizures in the foci of initiation, the primary SoCx layer 5.

1.4 Thesis Hypothesis and Objectives

Considering all that has been previously explained, AIS T-type calcium channels play a dominating role in spiking and bursting behaviour, and, therefore, they control neuronal transmission and in abnormal conditions could trigger absence seizures. Despite this fact, little is known about the intrinsic mechanisms of T-type burst firing and how upregulations lead to increased neurotransmission and synchronicity in a SoCx network. Therefore, computational neuroscience models are needed to give insight into mechanisms and parameters challenging to approach in vivo.

This thesis hypothesizes that an upregulation of the T-type calcium channels will increase burst firing events, thus increasing the synchronicity of a SoCx local network, which could trigger an absence seizure attack. In other words, this thesis aims to understand and give insight into T-type calcium channel bursting mechanisms and their effect on neurotransmission and absence seizures. For that, a compartmentalized integrate-and-fire model extended to include the mentioned channels and fitted with primary SoCx layer 5 pyramidal neuronal data has been designed and developed to prove the hypothesis. Furthermore, it has been connected with the two principal interneuron populations in the SoCx, which also play a vital role in inhibiting the AIS.

As far as we are concerned, these models will enable us to:

- Understand the intrinsic bursting mechanisms in the principal excitatory neurons and give us insight into the basic neural mechanisms underlying hypersynchronization states in the initiation foci of absence epileptic seizures.
- See if different networks with different configurations increase epileptogenesis susceptibility.
- Understand how T-type calcium currents affect neurotransmission for tackling a complex multi-nodal disease like epilepsy

This study could reduce the time-consuming and costly drug development pipeline to develop future potential therapeutics.

2 Methods

2.1 Neuronal Injection Inputs

2.1.1 Ornstein-Uhlenbeck Stochastic Process

In order to generate in vivo-like inputs, which represent spike trains arriving from different brain areas, Ornstein-Uhlenbeck processes are modelled. An Ornstein-Uhlenbeck process is a stochastic process that correspond to a coloured, gaussian, markovian and stationary noise [59]. In other words, it only depends on the previous state, it has a normal distribution, and mean and variance are constant over time [60]. This process is quite standard in computational neuroscience models and has been proved to generate in vivo-like inputs [60, 61, 62]. Ornstein-Uhlenbeck currents are determined in every time step by its Itô's calculus form (Eq. 1). Full derivation can be observed in Supporting Information S.I.

$$I(t+dt) = I(t) + \frac{\mu - I(t)}{\tau}dt + \sigma G_t \sqrt{\frac{2dt}{\tau}} \tag{1}$$

G_t is a random number sampled from a normal distribution function, with mean 0 and standard deviation 1, at each time step. The standard deviation (σ) and correlation time length (τ) are settled invariably at 300 pA and 3 ms, respectively. While the mean, μ, is assumed to be 100 pA in the interneuronal populations, it varies for the different layer 5 pyramidal cell compartments and simulations. Then, μ will be specified for each case. Parameters remain constant along the entire stochastic process, and the initial value for the Ornstein-Uhlenbeck process is assumed to correspond to the μ selected.

2.1.2 Oscillatory Poisson Process

The Poisson process is a stochastic process able to generate a point process with events being statistically independent. Therefore, it provides a valuable and good approximation to simulate stochastic neuronal firing as it could represent spike-train arrivals at the presynaptic compartment in neocortical neurons [63]. An oscillatory firing rate was applied to the process by concatenating gaussian distributions that follow Eq. 2. Then, it must be considered that the mean of the concatenated distribution depends on the frequency and that the centre of each normal distribution is the oscillatory period multiplied by the cycle number. Moreover, the sum of multiple Poisson processes is done to emulate better a real presynaptic input in a neuron localized in a local cortical synaptic network.

$$f(t) = \frac{1}{\sigma\sqrt{2\pi}} e^{-\frac{(x-\mu)^2}{2\sigma^2}} \tag{2}$$

It can be appreciated in Fig. 3 that the concatenated Gaussian distributions lead to an oscillatory spike-train as desired. Moreover, the dephase of the probability distributions affects the timing of the oscillatory firing rate.

This method is powerful as it enables the user to modulate inputs from different cortical areas like the SoCx. Here, the study of the neuronal excitability, spiking, and bursting mechanisms of a single neuron is done by applying this process. In fact, the Oscillatory Poisson process is used to see the AIS T-type calcium channel effects on the intrinsically bursting properties and, therefore, to see how it affects to elevated neurotransmission and

to seizure initiation. All parameters used in single-cell simulations will be specified in each case.

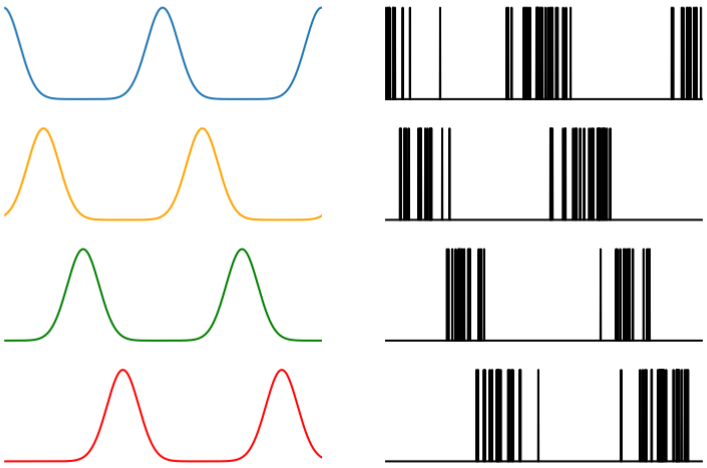

Figure 3: Oscillatory Poisson process input generation. In the left, there are four equal gaussian frequency probability distributions with different phases ($freq$ = 10 Hz, σ = 100, $gain$ = 50). The resulting spike trains appear on the right.

2.2 Single-cell and Ionic Channel Models

2.2.1 Layer 5 Somatosensory Cortex Pyramidal Model

As previously mentioned, this thesis aims to study excessive neurotransmission in the layer 5 of the SoCx, which could result in a hypersynchronous stage that triggers absence seizures. Therefore, there is a need to model pyramidal neurons, which are the most abundant excitatory cells in the mammalian cerebral cortex [64, 65]. As stated in the literature, even though there are strong family resemblances across the different pyramidal cells, their appearance and function vary depending on the nuclei. Moreover, it is known that neurons can be seen as a compartmentalized entity as they have differences in ion channel distributions and resting membrane potentials [66, 67]. Therefore, the model used is a compartmentalized integrate-and-fire based on the one published by Larkum et al. (2004), fitted to experimental data from primary SoCx layer 5 pyramidal neurons in rats [62]. The model compartments represent the dendritic tuft and the somatic compartment. This model enables us to integrate top-down and bottom-up activity to understand the single-cell neurotransmission integration in a network. The AIS is assumed to be inside the somatic compartment as this one triggers the spike. It could be seen as a plausible assumption as integrate-and-fire does not model explicitly the spiking dynamics. Furthermore, the neuronal division allows the model to incorporate the T-type calcium channel only in the AIS to see the intrinsic properties of the bursting and seizure initiation.

$$C_S \frac{dV_S}{dt} = \frac{1}{R_S}(V_{rest,S} - V_S) + \frac{1}{R_T}(V_D - V_S) + I_{AHP} + I_{T-type} + I_{Inject,S} \tag{3}$$

Where I_{AHP} can be described by the following equation:

$$I_{AHP} = g_{AHP}(E_K - V_S)e^{\frac{-t}{\tau_k}} \tag{4}$$

On the one hand, the somatic and AIS compartment (Eq. 3) has transient potassium afterhyperpolarization currents (AHP) activated when action potentials are emitted. As a matter of fact, different spikes activate different AHP currents due to being a calcium-activated potassium current, meaning that we can add them linearly. This current is modelled as a decay differential equation. The somatic and AIS compartment is where the spikes occur, and these are modelled by clamping the voltage for 1 ms to 10 mV and resetting to -52 mV each time the membrane potential exceeds the established threshold. The T-type injected current added into the model is explained in Section 2.2.2. All parameters used for the model are shown in Supporting Information S.II.1.

$$C_D\frac{dV_D}{dt} = \frac{1}{R_D}(V_{rest,D} - V_D) + \frac{1}{R_T}(V_S - V_D) + I_{HVA} + I_{Inject,D} \tag{5}$$

Where I_{HVA} can be described by the following equations:

$$I_{HVA} = g_{HVA}mh(E_{Ca} - V_D) \tag{6}$$

$$\frac{dm}{dt} = \frac{m_\infty - m}{\tau_m} \quad \text{with} \quad m_\infty = \frac{1}{1 + e^{Sm(V_D+9)}} \tag{7}$$

$$\frac{dh}{dt} = \frac{h_\infty - h}{\tau_h} \quad \text{with} \quad h_\infty = \frac{1}{1 + e^{Sh(V_D+21)}} \tag{8}$$

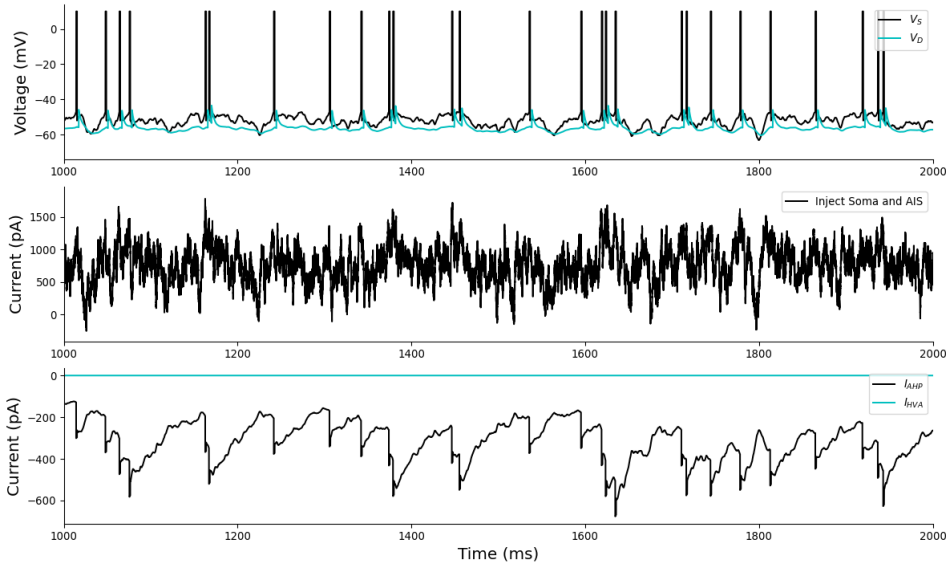

Figure 4: Response of the layer 5 pyramidal somatosensory neuron model to an Ornstein-Uhlenbeck injection in the somatic and AIS compartment of $\mu = 750$ pA. The upper graph shows compartment membrane potentials in time; black traces correspond to AIS and soma, and blue traces to the dendritic tuft. The middle graph corresponds to the injected current in time, and the below one to how HVA and AHP currents evolve in time. T-type conductance is set to 0 nS. It can be seen that the neuron exhibits a tonic firing behaviour with some burst due to the high injected current.

On the other hand, the dendritic compartment has a dendritic calcium channel that enables the model to fire long-lasting bursts, a different type of burst that is not mediated via Cav3 and that can be of interest for comparison purposes and to have a better insight into all the pyramidal neuron dynamics [67]. The dendritic calcium channel represents a high-voltage-gated (HVA) channel as it opens at relatively high membrane potentials. This dendritic current has an activation and inactivation channel gating variable, m and h, that follow first-order kinetics as detailed in Eq. 7 and Eq. 8. Whenever a spike occurs in the somatic and AIS compartment, a backpropagation action potential arrives at the dendritic tuft with a particular delay [68]. The assumption made to model backpropagation is that the dendritic membrane potential is artificially elevated 10 mV 3 ms after the spike occurs. The injected external currents will be specified for each case.

An injection in the somatic compartment leads to a tonic spiking behaviour of the pyramidal neuron. A tonic-like behavior appears because the injected current allows the compartment to overpass the threshold and then emit an AP, but backpropagation action potentials are not enough to activate the HVA dendritic calcium channels. Therefore, long period bursts are not achieved. Moreover, as shown in Fig. 4, the afterhyperpolarization current decreases once a spike occurs because the membrane potential is becoming less hyperpolarized.

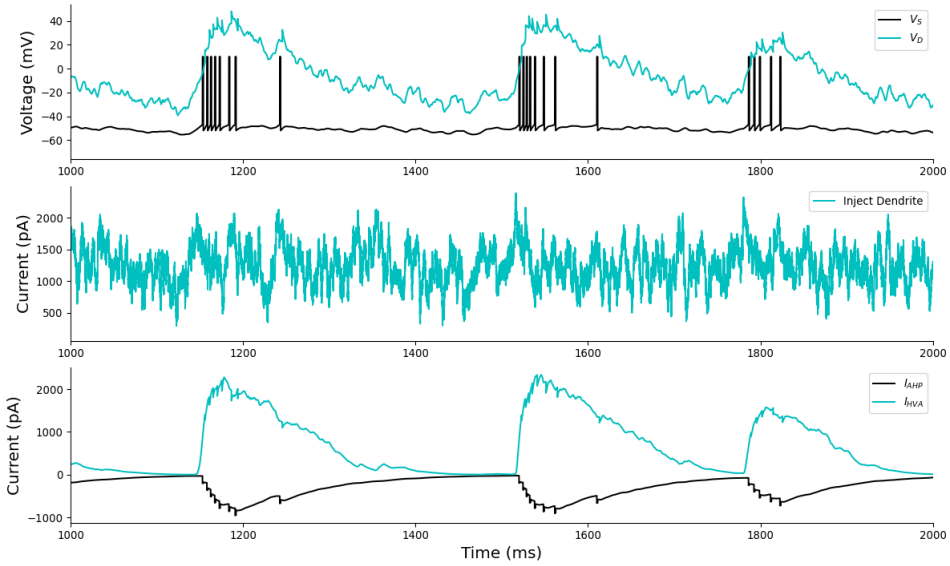

Figure 5: Response of the layer 5 pyramidal somatosensory neuron model to an Ornstein-Uhlenbeck injection in the dendritic compartment of $\mu = 1250$ pA. The upper graph shows compartment membrane potentials in time; black traces corresponds to AIS and soma, and blue traces to the dendritic tuft. The middle graph corresponds to the injected current in time, and the below one to how HVA and AHP currents evolve in time. T-type conductance is set to 0 nS. It can be seen that the neuron exhibits long bursting behaviour due to the activation of HVA calcium currents.

Secondly, as seen in Fig. 5, an injection in the dendritic compartment lead to burst firing in the pyramidal neuron. This phenomenon happens because the external current enables the activation of the dendritic calcium channels, leading to a long activation period [21]. These bursts are different from those generated by Cav3, as they are long period bursts instead of low period spike bursts.

On top of that, the relation between the mean injected current, and the mean firing rates are computed to know how channels and currents affect the spiking dynamics, as shown in Fig. 6. It is seen that the dendritic calcium channels are responsible for the burst spiking that can be appreciated in Fig. 5 since, without them, the number of spikes dramatically decays. Moreover, APs seem to increase when the somatic current injection is increased, leading to a correlation between both phenomena. In addition, as can be seen from Fig. 6, when the two sources of input coincide in time, the neuron gain increases, which is relevant as it represents different input arrivals in the presynaptic area.

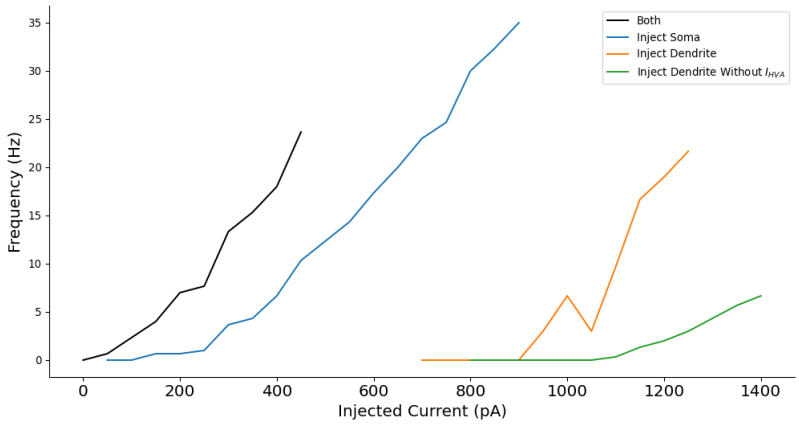

Figure 6: Layer 5 pyramidal somatosensory neuron frequency with respect to the input. All inputs were modelled with an Ornstein-Uhlenbeck stochastic process. It can be seen that more significant intakes are correlated with higher fire frequencies. Moreover, if inputs coincide in time in the different compartments, the gain is increased as stated by Larkum [62]. It can also be observed that without HVA, the firing rate decays consistently as the neuron cannot fire long-lasting bursts without a dendritic injection.

All in all, it represents an accurate model to represent the top-down and bottom-up integration activity of layer 5 pyramidal cells and allows us to study the effects of AIS T-type calcium channels either in single-cell or network environments.

2.2.2 The AIS T-type Calcium Channel Model

As mentioned above, the study of AIS T-type calcium channels is essential as they are a valuable contributor to neuronal excitability and to burst firing [69]. Upregulation of these channels could lead to increased network synchronization and, therefore, to seizure initiation. In order to be able to model these channels, we have to consider their properties to emulate their role and function. As stated by the name, these transient channels are activated at relatively hyperpolarized membrane potentials, thus having only a small range where they can be activated but without being completely inactivated. T-type calcium currents inactivate rapidly during maintained depolarization yet recovers slowly from inactivation.

The model used is based on the one presented by Huguenhard and McCormick but adapted to represent the AIS T-type calcium channels from layer 5 SoCx pyramidal cells [70, 71]. Even though this model is relatively standard in literature and has been used so far to represent T-type currents in different neuronal populations, nobody has previously used

to emulate T-type channels in the SoCx or the AIS T-type calcium channels [72, 73, 74, 75].

Parameters regarding the gating variables and gating dynamics have been adapted by considering multiple experimental studies about T-type current properties in the cortex that found consistent results [39, 76, 77, 78]. These previous studies show that the activation threshold and the recovery time differed between neuronal populations. Data used comes from Chemin et al. (2002) Cav3.2 channel experiments as Cav3.2 is the one that is more present in the AIS and that affects more to seizure initiation [39, 78]. This model is introduced in the somatic and AIS compartment from the Layer 5 primary SoCx pyramidal neuron model. All parameters used for simulations are shown in Supporting Information S.II.2.

$$I_{T-type} = g_T m^2 h (E_{Ca} - V_S) \tag{9}$$

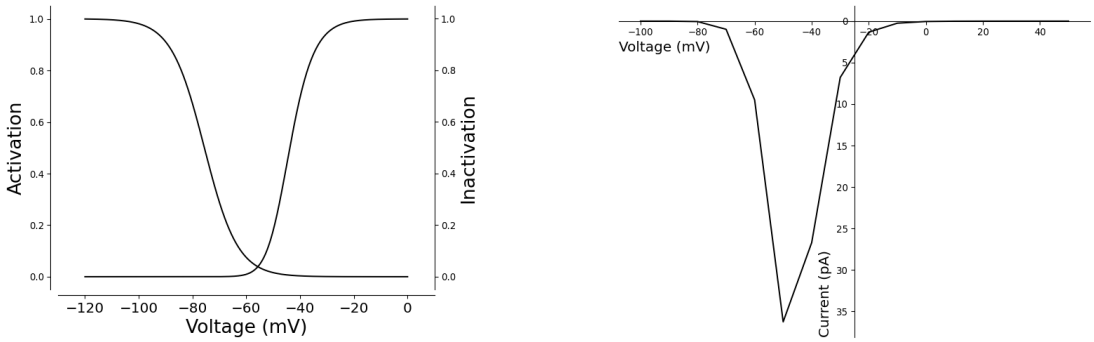

(a) **(b)**

Figure 7: AIS T-type calcium channel properties. (a) Activation and inactivation channel gating variables. It can be seen that the window current starts from around -70 mV. (b) Maximal current with respect to stationary membrane potentials, considering $g_T = 75$ nS. It shows the current window.

Steady-state activation and inactivation gating variables were modelled with a Boltzmann-style equation, assuming that there was a uniform population of channels that can be described by the mentioned equation [70]. The activation variable is faster, as shown in Eq. 9, thus facilitating the generation of long LTS Ca2+ spikes, which could answer why the channel triggers bursting mechanisms.

$$\tau_m = \frac{1}{e^{\frac{V_S+132}{-16.7}} + e^{\frac{V_S+16.8}{-18.2}}} + 0.612 \tag{10}$$

The activation time constant, Eq. 10, is described as a bell-shaped function (See Fig. 8), similar to the ones seen for Na+ and K+ currents by Hodgkin and Huxley [79].

$$\tau_h = e^{\frac{V_S+22}{-10.5}+28} \quad \text{if} \quad V_S >= -70mV \tag{11}$$

$$\tau_{rec} = e^{\frac{V_S+467}{66.6}} \quad \text{if} \quad V_S < -70mV \tag{12}$$

As seen in Eq. 11 and Eq. 12, inactivation kinetics are biphasic as recovery from inactivation occurrs at much slower rates than current inactivation. Recovery can be modelled, as seen, as a monoexponentially process.

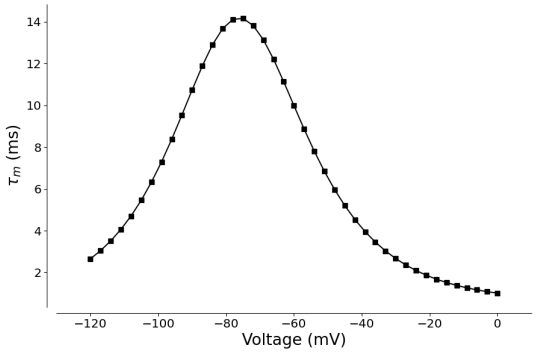

Figure 8: AIS T-type calcium channel activation time constant with respect to voltage. It is seen that it follows a bell-shaped form.

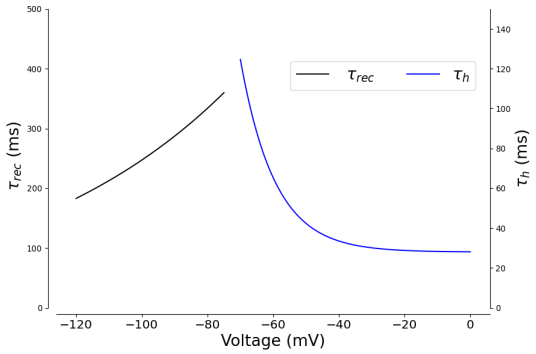

Figure 9: AIS T-type calcium channel biphasic inactivation kinetics with respect to voltage. It is seen that recovery can be modelled as a monoexponential process.

2.2.3 Parvalbumin Fast-Spiking Interneuron

Parvalbumin (PV) positive interneurons are the most abundant gamma-aminobutyric acid-producing (GABA) inhibitory interneurons in the neocortex, and in the primary somatosensory area [80, 81]. These cells are named PV due to their expression of the non-overlapping calcium-binding parvalbumin protein [82]. PV interneuron is characterized to be rapidly activated and produce brief spikes, thus regulating the excitatory neuron with millisecond-level precision via inhibition [83]. Then, these interneurons are characterized by a fast-spiking physiological phenotype with high and fast AHP currents [80, 84]. Moreover, they are characterized by low resting potentials, rapid conductances and membrane kinetics, low input resistances, and for presenting no spiking-frequency adaptation [82]. All these characteristics allow the neuron to fire precisely timed spikes at high rates [81].

Considering all the electrophysiological properties of PV, it was decided to use the Izhikevich fast-spiking interneuron model as it reproduces rat PV cortical interneuron spiking

behaviour and it considers that fast-spiking interneurons have an absence of rebound response [85].

$$20\frac{dv}{dt} = (v + 55)(v + 40) - u + I_{Inject,PV} \tag{13}$$

$$\frac{du}{dt} = 0.2(U(v) - u) \tag{14}$$

The model consists of two differential equations: a fast voltage variable (Eq. 13) and a slow recovery from the inactivation variable (Eq. 14). The interneuron AHP spike is modelled by setting the fast voltage variable to -45 mV once it overpasses an established threshold of 25 mV. The slow nonlinear nullcline, $U(v)$, is modelled with, $U(v) = 0$ when $v \geq v_b$ and $U(v) = 0.025(v\text{-}v_b)^3$ otherwise, with v_b = –55 mV. This nonlinear nullcline allows us to take into account the lack of rebound spikes in PV interneurons.

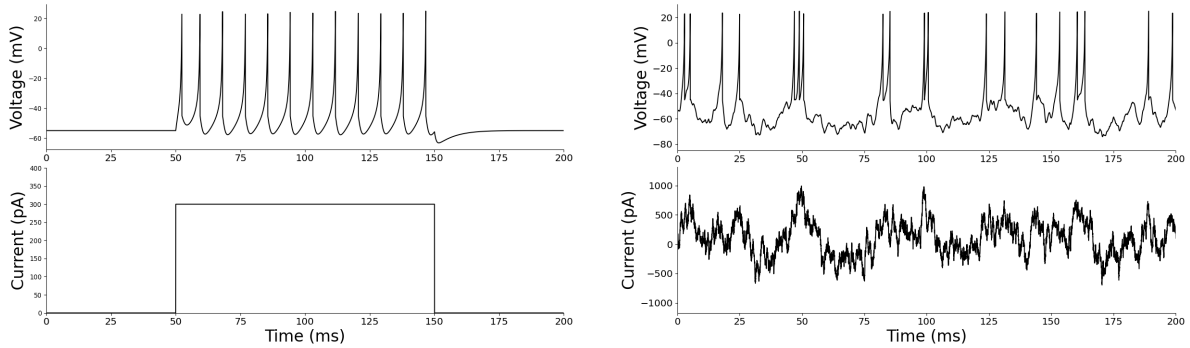

(a) **(b)**

Figure 10: PV-expressing interneuron response to different inputs. (a) Response to a square-pulse injected current of 300 pA. (b) Response to an Ornstein-Uhlenbeck stochastic noise input of μ = 100 pA.

In Fig. 11, we can appreciate that the model represents what happens experimentally in the rat cortex's PV interneuron, as there is no spike-adaptation to frequency.

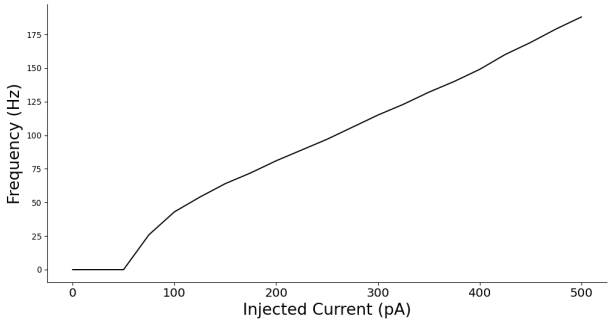

Figure 11: PV-expressing interneuron firing frequency with respect square-pulse injections.

2.2.4 Somatostatin Low-Threshold Spiking Interneuron

Somatostatin (SOM) positive interneurons are the second most abundant GABA interneurons in the neocortex, and in the primary SoCx [80, 81]. These cells are named SOM due

to their expression of the non-overlapping somatostatin peptide [83]. These interneurons are characterized by requiring repetitive, facilitating, and afferent inputs to be activated, thus being involved in dendritic integration and preventing pyramidal hyperactivation [83, 86]. They are present in the layer 5 of the cortex and are known to have low-threshold spiking (LTS) dynamics. Therefore, even though the input resistance and resting potentials are higher in SOM than in PV interneurons, they have a slower time constant [82]. Another difference compared with the previous interneuron is that it can show rebound spiking and a slow spike-frequency adaptation. All in all, it shows regular spiking patterns in response to injected pulses. Furthermore, low-frequency subthreshold oscillations in membrane potential can be seen after weak depolarization.

Considering all the electrophysiological properties of SOM, it was decided to use the Izhikevich LTS interneuron model as it can reproduce rat SOM cortical interneuron spiking behaviour [85].

$$100\frac{dv}{dt} = (v+56)(v+42) - u + I_{Inject,SOM} \tag{15}$$

$$\frac{du}{dt} = 0.03(8(v+56) - u) \tag{16}$$

The model consists of two differential equations: a fast voltage variable (Eq. 15) and a slow recovery from the inactivation variable (Eq. 16). It is assumed that the spike peak and resetting point depend on the slow recovery variable to consider decreasing changes in AHP and spike amplitudes. Therefore, if $v \geq 40 - 0.1u$, then $v \leftarrow -53 + 0.04u$ and $u \leftarrow \min(u + 20, 670)$. This last assumption does not affect much to neuronal excitability but gives a more realistic voltage trace in comparison with experimental data.

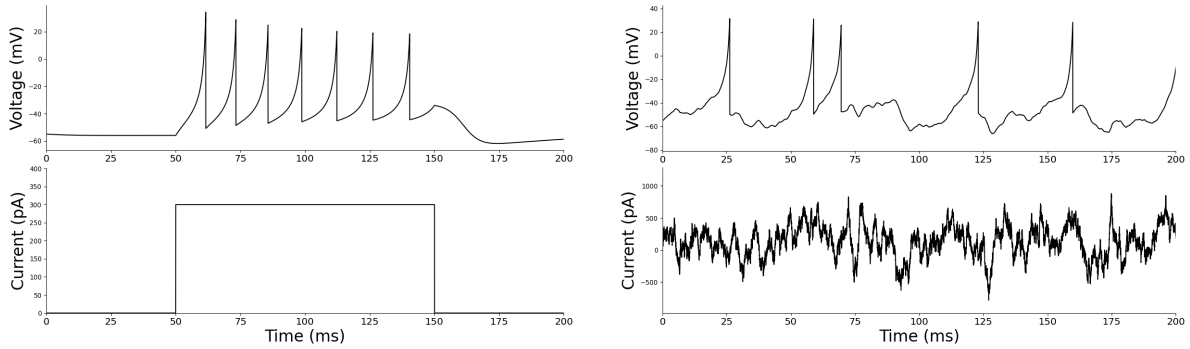

(a) **(b)**

Figure 12: SOM-expressing interneuron response to different inputs. (a) Response to a square-pulse injected current of 300 pA. (b) Response to an Ornstein-Uhlenbeck stochastic noise input of $\mu = 100$ pA.

In Fig. 13, we can appreciate that the model represents the f/I plot of a SOM interneuron of the rat cortex. As expected, if not significant inputs are applied, the slow spike-frequency adaptation is not seen.

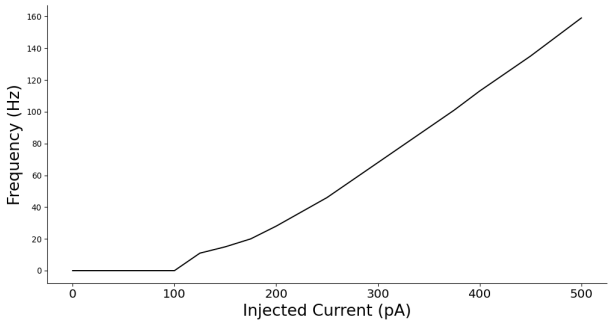

Figure 13: SOM-expressing interneuron firing frequency with respect to square-pulse injections.

2.3 Primary Somatosensory Cortex Network

As previously mentioned, there is the need to model the local primary SoCx network to observe how changes in the AIS T-type calcium channels and neuronal excitability affect the network synchronization and why these changes are responsible for seizure initiation. For that, we use the models described above about the principal excitatory neurons, layer 5 pyramidal cells, and the two main GABA interneurons, which play a significant role in regulating neuronal excitability and oscillation [87]. The SoCx network dynamics and connection schematics can be observed in Fig. 14. It must be considered that each neuronal type receives an Ornstein-Uhlenbeck process to model the connections with other neurons or cortical areas outside the network [81]. PV and SOM expressing interneurons have an Ornstein-Uhlenbeck process with a mean of 100 pA. Layer 5 pyramidal Ornstein-Uhlenbeck processes will be specified in every simulation as it is changed for comparison purposes.

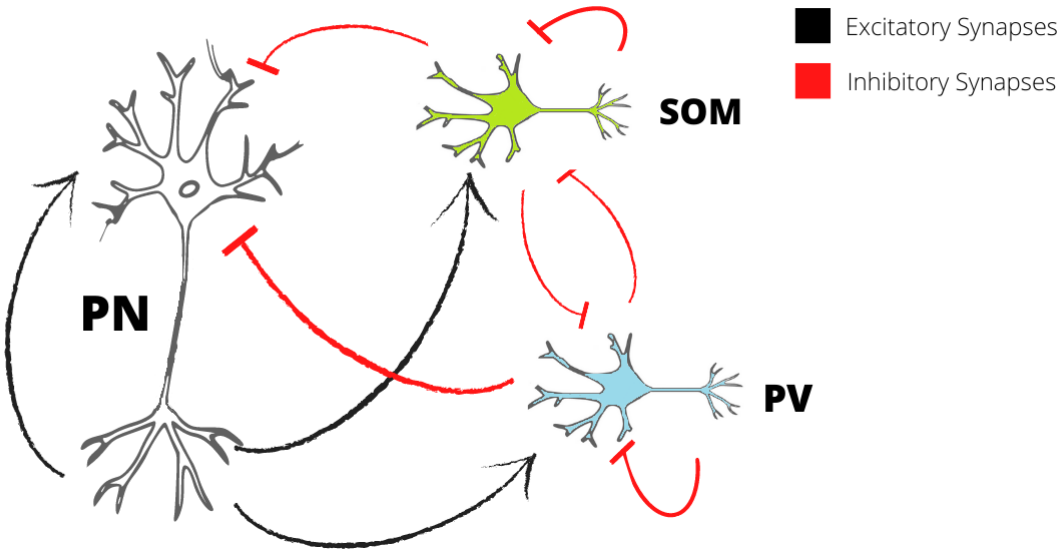

Figure 14: Primary somatosensory cortex layer 5 network schematics and dynamics.

Each network is composed of a total of 1000 neurons. As stated in the literature, around 80% of the cortex corresponds to excitatory pyramidal neurons [86, 88]. Then, each network is constructed with 800 deep-layer pyramidal cells, 100 PV-expressing, and 100 SOM-

expressing interneurons. The different neuronal populations are coupled by conductance-based synapses, following Eq. 17.

$$I_{syn} = \sum_i g_{syn} \exp\left(-\frac{t - t_i}{\tau_{syn}}\right)(V - E_{syn}) \tag{17}$$

A decaying exponential differential equation, equal to Eq. 17, models synapses in the postsynaptic neuron. The excitatory conductance is set to $g_{syn,e}$ = 2 nS and the time constant to $\tau_{syn,e}$ = 2.5 ms. As seen in previous experimental and theoretical works, the inhibitory synapse has a stronger conductance and recovers more slowly than the excitatory ones [89, 90]. Then, the inhibitory conductance is set to $g_{syn,i}$ = 3 nS and the time constant to $\tau_{syn,e}$ = 5 ms. The reversal potentials for excitatory and inhibitory synapses are $E_{syn,e}$ = 0 mV and $E_{syn,i}$ = -75 mV, respectively. Moreover, an axonal delay of 2 ms in neuronal transmission is considered to be more realistic. In Eq. 17, the first term corresponds to the presynaptic neurons, and the other corresponds to the postsynaptic one, thus enabling the transmission of excitability. All simulations, unless specified, have a simulation time of 3 ms. The first 0.5 seconds are neglected as they are considered transient.

2.3.1 Network Connectivity

It is well-known that the connectivity differs between different local SoCx synaptic networks; therefore, oscillations will change across different local areas. Beta (12-30Hz) and Gamma (30-100Hz) rhythms have been seen to be quite common in the somatosensorial area [91, 92, 93, 94]. In fact, they have been related to different somatosensorial processes such as perception of pain and cognitive processes [94]. More importantly, as mentioned before, increased local beta and gamma rhythms have been seen and correlated in patients during ictal and interictal phases of the absence seizures [7, 13]. Then, as epilepsy is a multi-nodal disease resulting from excessive neuronal excitation, it is vital to understand why upregulations in the T-type calcium channel lead to seizures in SoCx networks and if some network configurations promote epileptogenesis [65]. Considering that network activity is generated due to balances between the population and connection of neurons, different network configurations have been proposed to emulate different real cortical networks [95]. Before entering in details about the connectivity matrices, some experimental data was considered. Layer 5 pyramidal cells are known to be highly connected among themselves and are also connected to interneuron types [81]. PV-expressing interneurons are connected to PV and to the soma of pyramidal cells, thus controlling action potential summation, but are not connected to other interneurons [86, 96]. SOM-expressing interneurons target the dendrites from pyramidal cells, inhibit other interneurons and inhibit themselves weakly [83, 96].

As it is known that PV-expressing interneurons regulate gamma rhythms and SOM-expressing interneurons regulate beta rhythms, two configurations of the net have been used to give each interneuron a dominating role [86, 87]. Moreover, other two types of nets, symmetrically coupled connectivity net and only pyramidal net, have been proposed. A symmetrically coupled network could give us an insight into networks where the two subtypes operate equally and the pyramidal one in networks where interneurons are not present, which has also been linked to epilepsy [65]. See Tables 1 and 2 for details on the connectivity probabilities used.

		From					
		SOM Net			PV Net		
		PYR	PV	SOM	PYR	PV	SOM
To	PYR	0.1	0.01	0.15	0.1	0.15	0.01
	PV	0.01	0.05	0.05	0.05	0.01	0.01
	SOM	0.05	0.0	0.01	0.01	0.0	0.05

Table 1: Connectivity for the SOM and PV dominating networks. Connectivity is expressed as the probability of a presynaptic neuron being connected with the correspondent postsynaptic one.

		From					
		SC Net			PYR Net		
		PYR	PV	SOM	PYR	PV	SOM
To	PYR	c	c	c	0.1	0	0
	PV	c	c	c	0	0	0
	SOM	c	c	c	0	0	0

Table 2: Connectivity for the symmetrically coupled and pyramidal network. Connectivity is expressed as the probability of a presynaptic neuron being connected with the correspondent postsynaptic one. The parameter c corresponds to 0.1 or 0.05, depending on the simulation.

2.4 Network Analysis

2.4.1 Spike and Bursting Metrics

Bursts are defined as events of consecutive spikes with an interval spiking time shorter than 5 ms as stated in previous theoretical studies [26, 97]. It is considered that multiple spikes can form bursts events and that there are different burst types. With respect to the metrics calculated, the mean of burst events was done with 8000 pyramidal cells, each one with different connectivity to see the averaging burst per pyramidal layer 5 neuron in the SoCx and see how AIS T-type calcium channels modifies it in simulations. Error bars were represented as the mean ± the standard deviation.

2.4.2 Spectral Analysis

On the one hand, to see the oscillatory and synchrony patterns of the net, we compute the Power Spectral Density (PSD) using the Multitaper and windowing method. This method, introduced by David J. Thomson in 1988, has been seen to be relatively accurate in analysing neural time data as it overcomes the limitations of the conventional Fourier analysis in noisy signals [98, 99]. The PSD is computed for the summed pyramidal spike trains and averaged among ten trials. Trials are defined as different network simulations, including the generation of new connectivity matrices and inputs. The window size used is 1000 samples, and it is moved in steps of 10 elements. Each window is symmetrically padded with zeros until a final length of 4096.

On the other hand, time-frequency analysis were also performed using the previous method for frequency components. It is assumed that the frequency components of each window

represent the frequency components at the centre of the window [99].

2.5 Technical Information

Mathematical models were numerically integrated by using the Forward Euler Method with a time step of 0.1 ms. Julia Programming Language 1.5.3[1] was used to simulate all that is presented in this thesis. The only exception was the spectral methods that were implemented in the Spyder 4.0.1[2] environment using Python 3.7.6[3] to be able to use the ScyPy package needed to compute the Slepian functions.

The Julia 1.5.3 packages needed to reproduce the data and results obtained are Pkg, Parameters, Random, Distributions, FFTW, PyCall, PyPlot, Profile, and DelimitedFiles.

The Python 3.7.6 packages needed to reproduce the data and results obtained from the spectral methods are Numpy, Future, Os, Pandas, SciPy, Datetime, Operator, Warnings, and Matplotlib.

All code used is available at the Dynamical Systems Biology laboratory GitHub repository[4].

[1] https://julialang.org/
[2] https://www.spyder-ide.org/
[3] https://www.python.org/
[4] https://github.com/dsb-lab/BTs_Tomas_Berjaga_Buisan

3 Results

All results in this thesis are extracted following the methods section explained above (See Section 2). Further results and information about them can be checked at Supporting Information (See Supporting Information S.III).

3.1 AIS T-type Calcium Channels Trigger Burst Firing

On the one hand, in Fig. 15, it can be appreciated that without the action of the AIS T-type calcium channels, the excitatory neuron fires single-tonic spikes when a Poisson Process (f = 10 Hz, σ = 100, gain=30), resulting from the sum of 50 single Poisson processes (each with a different dephase), is considered in the AIS and somatic compartment. As seen in Fig. 15, backpropagation spikes are not enough to activate the HVA dendritic calcium channels either.

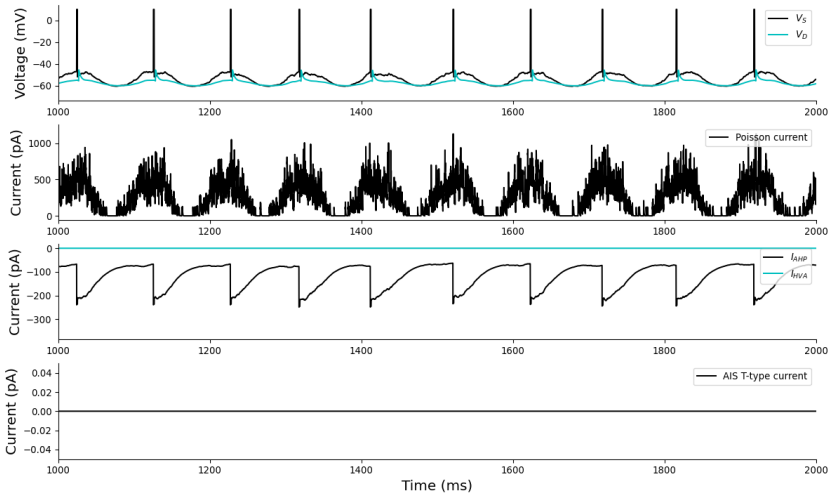

Figure 15: AIS T-type calcium channel effect on firing behaviour. The upper graph shows compartment membrane potentials in time; black traces corresponds to the AIS and soma, and blue traces to the dendritic tuft. In the middle graphs, one corresponds to the injected current in time, and the other to how HVA and AHP currents evolve in time. And the last one to the AIS T-type current with g_T = 0 nS.

On the other hand, in Fig. 16, it can be observed that the action of AIS T-type calcium channels leads to the firing of consecutive spikes each time the membrane potential is in the T-type calcium channel activation window. Consecutive spikes could be considered as burst if they have an interval spiking time below 5ms [26, 97]. Therefore, it is fair to say that the action of these channels is promoting bursting as it is appreciated that consecutive spikes are formed as the ones seen in experimental studies [52, 56, 100]. AIS T-type calcium channel behaviour matches with experimental data as it is demonstrated their main hallmark; they reach a peak and then decay as they are transient currents [39]. Moreover, an increase in T-type currents is correlated with increases in AHP current amplitudes, which happens in our results as observed in Fig. 16 [57]. Furthermore, the AIS T-type calcium channel properties must be considered to understand the current peak amplitude. T-type calcium channels have a slow recovery time; therefore, if the activation frequency is elevated, the channel will not have time to be recovered entirely to fire with maximal potency. Then, it is fair to say that they will resonate better at low frequencies. The same Poisson process has been applied to compare both results.

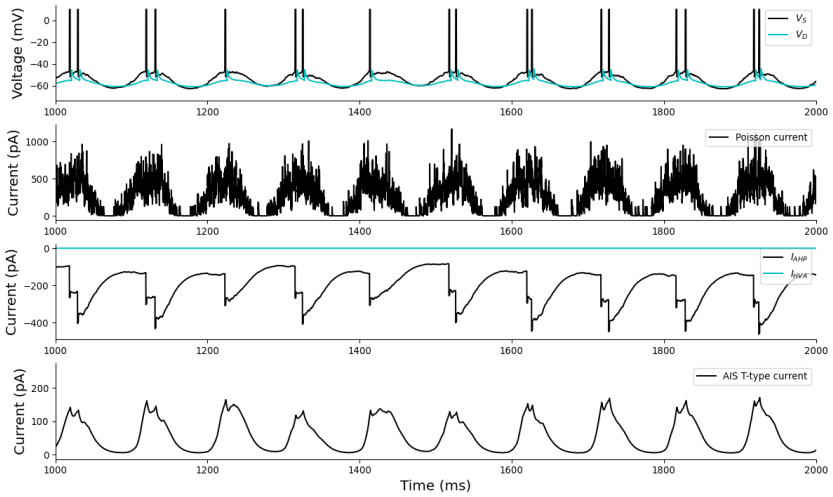

Figure 16: AIS T-type calcium channel effect on firing behaviour. The upper graph shows compartment membrane potentials in time; black traces corresponds to the AIS and soma, and blue traces to the dendritic tuft. In the middle graphs, one corresponds to the injected current in time, and the other to how HVA and AHP currents evolve in time. And the last one to the AIS T-type current with $g_T = 75$ nS.

3.2 AIS T-type Calcium Channels Promote Primary Somatosensory Layer 5 Synchronicity

3.2.1 Pyramidal Network

The pyramidal network comprises excitatory pyramidal neurons from the layer 5 of the primary SoCx, modelling networks where GABA interneurons are not connected or have a deficiency. The multitaper power spectrum has demonstrated that upregulations of the AIS T-type calcium channel lead to a considerable increase in pyramidal synchronicity (Fig. 17).

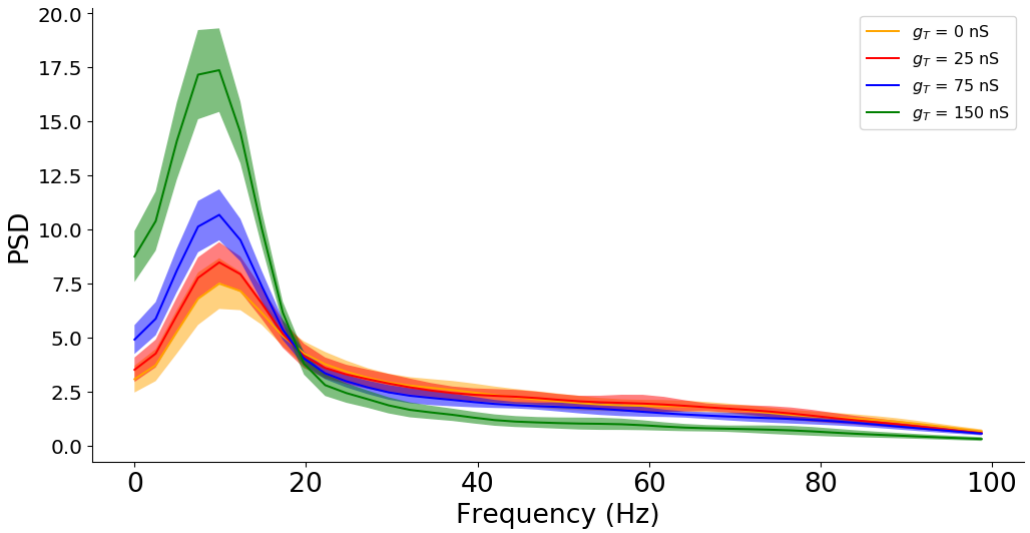

Figure 17: Pyramidal network multitaper power spectrum for different AIS T-type calcium conductances. As observed, elevated T-type calcium channel conductances increase the alpha oscillatory signal power and its synchronicity.

Hypersyncrhonizaton correlates with an augment in single-cell bursting events (Fig. 18). Therefore, as hypothesized in previous experimental studies, an increase in AIS T-type calcium channel performance increase bursting firing, thus, promoting network synchronicity [39, 50, 52]. Furthermore, the AIS T-type calcium channel does not change the oscillatory pattern or frequency band; it only promotes its synchronicity.

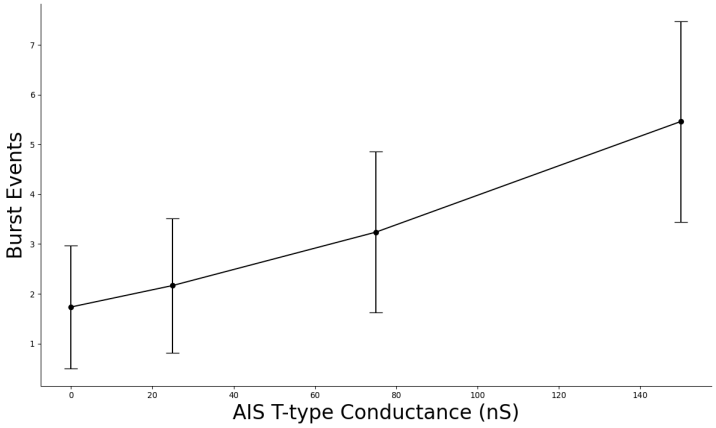

Figure 18: Pyramidal network burst events per simulation for different AIS T-type calcium conductances. As observed, elevated T-type calcium channel conductances increase bursting events in pyramidal cells. Each point in the plot is an average of 8000 pyramidal cells. Error bars were represented as the mean ± the standard deviation.

All this can also be seen in the time-frequency plots (Fig. 19), where conductance increases ensure synchronization, close to the main oscillatory frequency band, in time. These simulations were performed with an Ornstein-Uhlenbeck injection with a mean of 250 pA in both compartments of the excitatory pyramidal neuron.

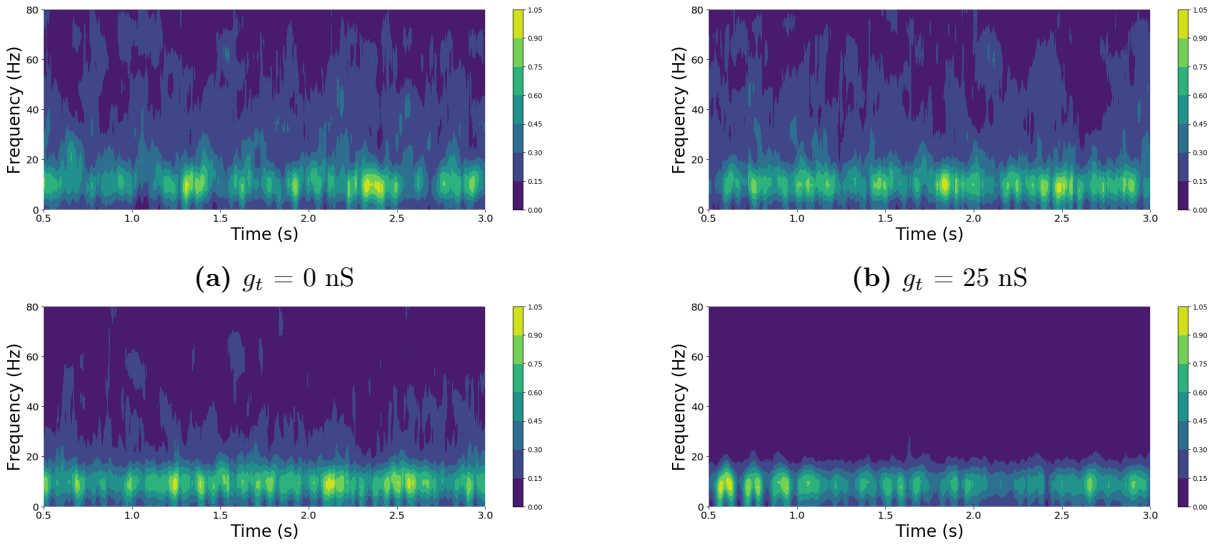

(a) $g_t = 0$ nS **(b)** $g_t = 25$ nS

(c) $g_t = 75$ nS **(d)** $g_t = 150$ nS

Figure 19: Pyramidal network time-frequency plots for different AIS T-type calcium conductances. An increase in condutance lead to a more synchronized activity.

3.2.2 SOM-dominating Network

The SOM-dominating network comprises excitatory pyramidal neurons from the layer 5 of the primary SoCx and the two main GABA interneurons, but SOM-expressing interneurons play a significant role among the interneuronal subtypes. As seen in experimental data, this net oscillates at the beta range [82, 86, 87]. The multitaper power spectrum shows that high AIS T-type calcium channel conductances increase power and synchronization in the pyramidal layer 5 neurons (See Fig. 20), correlating it with an augment in the number of bursts per cell. As stated above, increases in conductance lead to increases in synchronicity mediated by burst firing. Also, the oscillatory beta band was not disturbed by the channel action.

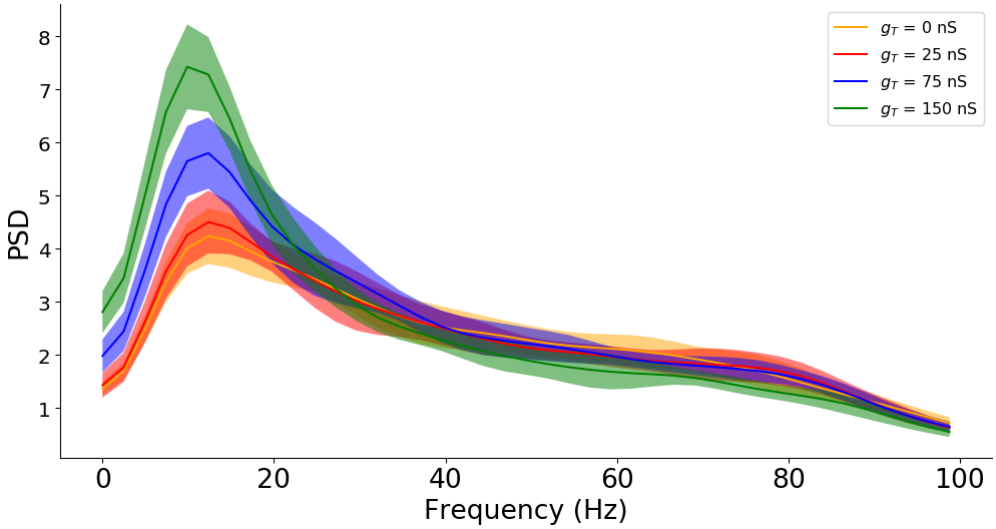

Figure 20: SOM-dominating network multitaper power spectrum for different AIS T-type calcium conductances. As observed, elevated T-type calcium channel conductances increase the beta oscillatory signal power and its synchronicity.

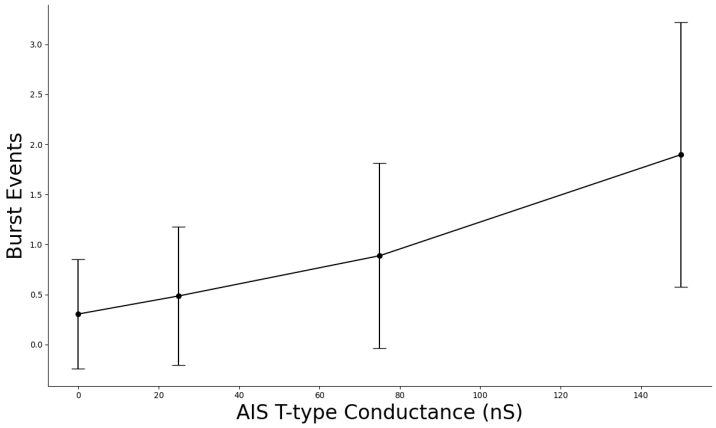

Figure 21: SOM-dominating network burst events per simulation for different AIS T-type calcium conductances. As observed, elevated T-type calcium channel conductances increase bursting events in pyramidal cells. Each point in the plot is an average of 8000 pyramidal cells. Error bars were represented as the mean ± the standard deviation. Consider that burst events below zero are non realistic.

Time-frequency plots show similar results, as bursting is ensuring synchronicity in time. These simulations were performed with an Ornstein-Uhlenbeck injection with $\mu = 250$ pA in both compartments of the excitatory pyramidal neuron.

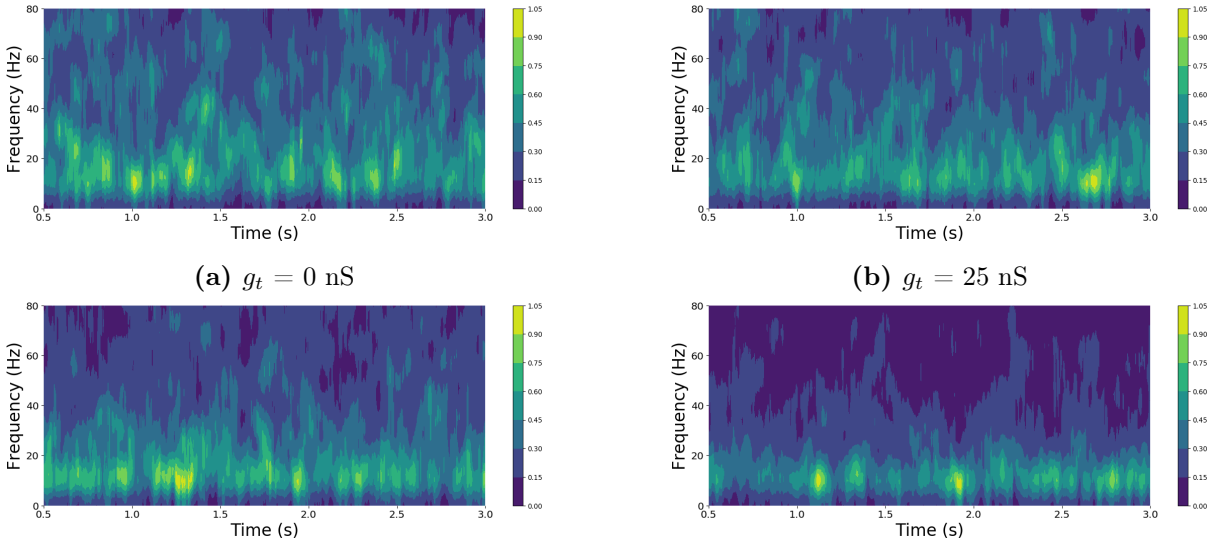

(a) $g_t = 0$ nS **(b)** $g_t = 25$ nS

(c) $g_t = 75$ nS **(d)** $g_t = 150$ nS

Figure 22: SOM-dominating network time-frequency plots for different AIS T-type calcium conductances. An increase in condutance lead to a more synchronized activity.

3.2.3 PV-dominating Network

The PV-dominating network comprises excitatory pyramidal neurons from the layer 5 of the primary SoCx and the two main GABA interneurons, but PV interneurons play a significant role among the interneuronal subtypes. Gamma oscillatory patterns arise from this network, as seen in experimental data [82, 87].

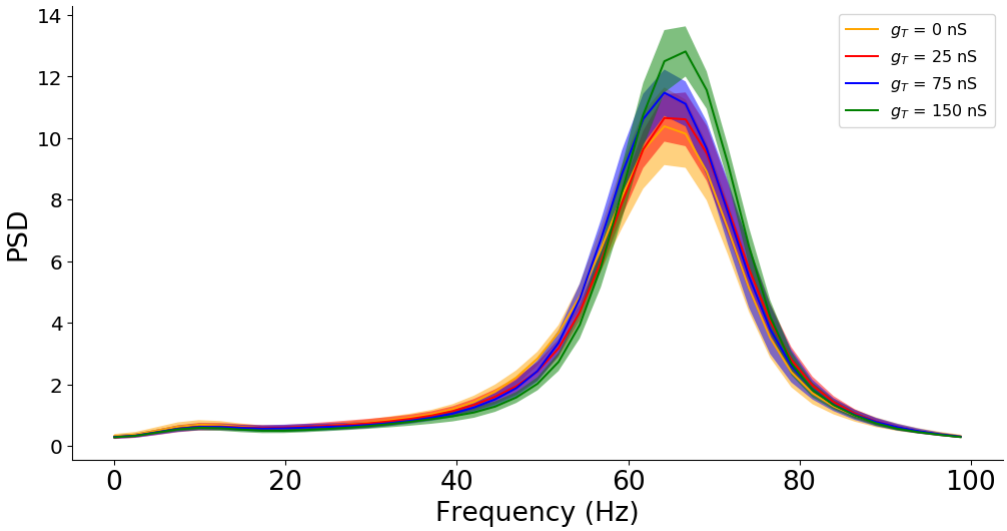

Figure 23: PV-dominating network multitaper power spectrum for different AIS T-type calcium conductances. As observed, elevated T-type calcium channel conductances increase the gamma oscillatory signal power and its synchronicity.

The multitaper power spectrum shows that an increase in channel conductance leads to an increase in synchronization. Despite this fact, slight changes are seen in this regime, resulting from the high input voltage (Ornstein-Uhlenbeck of $\mu = 750$ pA) needed to observe the oscillatory pattern. Moreover, AIS T-type calcium channels increase bursting behaviour, as seen in Fig. 24, but the relative change is not as significant as in previous cases as a high stochastic pattern is inferring huge injections leading to bursts. Therefore, it is fair to say that AIS T-type calcium channel performance is more noticeable in low-input networks.

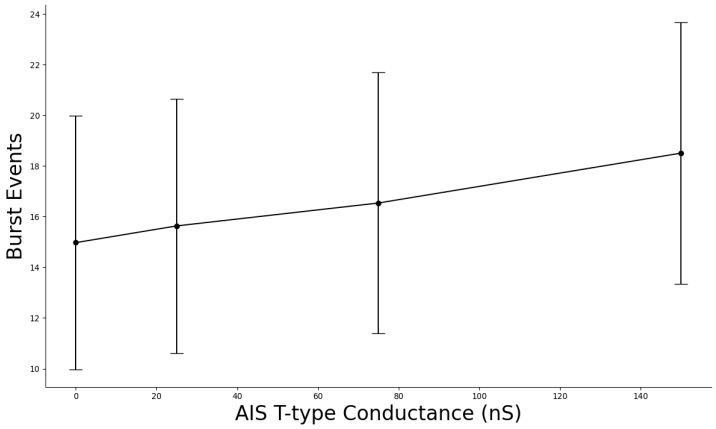

Figure 24: PV-dominating network burst events per simulation for different AIS T-type calcium conductances. As observed, elevated T-type calcium channel conductances increase bursting events in pyramidal cells. Each point in the plot is an average of 8000 pyramidal cells. Error bars were represented as the mean ± the standard deviation.

The time-frequency plots show similar results, as bursting is ensuring a little increase in synchronicity in time. These simulations were performed with an Ornstein-Uhlenbeck of $\mu = 750$ pA in both compartments of the excitatory pyramidal neuron as there is a need for high inputs to generate gamma oscillations.

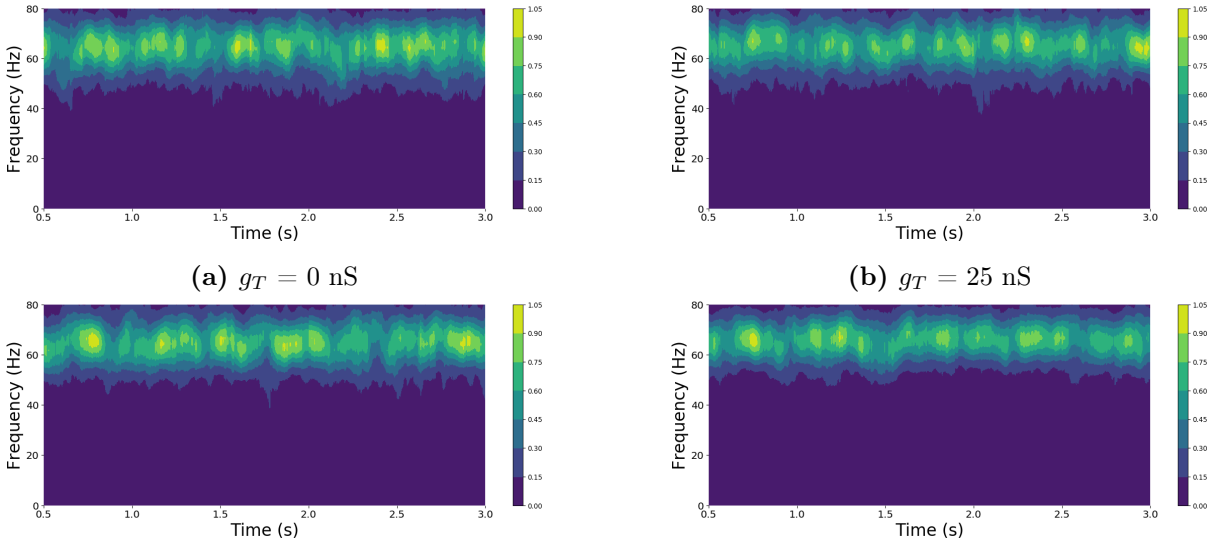

(a) $g_T = 0$ nS **(b)** $g_T = 25$ nS

(c) $g_T = 75$ nS **(d)** $g_T = 150$ nS

Figure 25: PV-dominating network time-frequency plots for different AIS T-type calcium conductances. An increase in condutance lead to a more synchronized activity.

3.2.4 Symmetrically Coupled Network

The symmetrically coupled network comprises a net where excitatory and inhibitory populations are connected equally with a probability of 0.1. It can be observed in Fig. 26 that as the two interneurons play a role in the pyramidal oscillatory dynamics, it has two oscillatory bands, at beta and gamma. It can be seen that the increase in AIS T-type calcium channel conductance has a more significant impact on the synchronicity of low frequencies than in the high frequencies. This fact could be related to gamma oscillations appearing in networks where there are high inputs. In fact, as an Ornstein-Uhlenbeck is applied, spike trains representing bursting events can be the presynaptic pyramidal input. These simulations were performed with an Ornstein-Uhlenbeck injection with a mean of 750 pA in both compartments of the excitatory pyramidal neuron as there is a need for high inputs to generate gamma oscillations.

Further information about this network and its time-frequency and burst event plots (that show similar results as above) can be seen in the Supporting Information S.III.3.

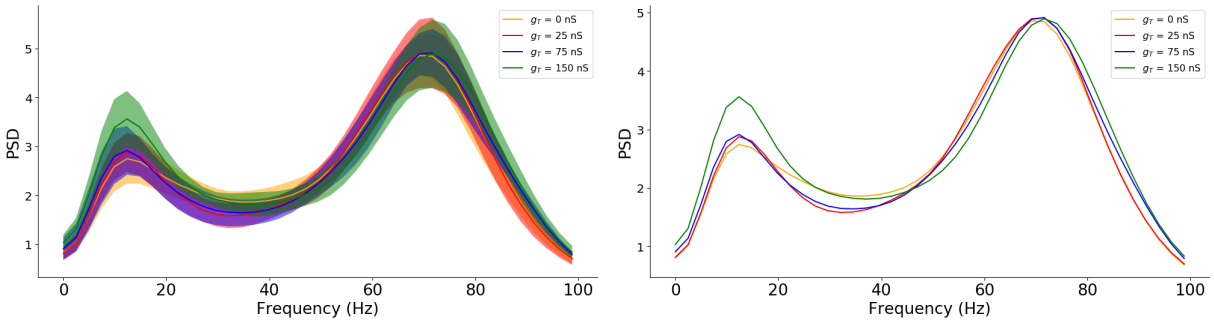

(a) **(b)**

Figure 26: Symmetrically coupled network multitaper power spectrum for different AIS T-type calcium conductances. As observed, elevated T-type calcium channel conductances increase the oscillatory signal power. (a) Multitaper power spectrum range and mean for 10 simulations. (b) Multitaper power spectrum mean for 10 simulations.

4 Discussion

The aim of this thesis was to gain insight into the fundamental brain hypersynchronization states that trigger the absence seizures start in the primary SoCx. This could help us understand the feedback disruptions between the SoCx and the thalamus that lead to the generation of the well-known SWD. To tackle this issue, the study of the T-type calcium channel in the neuronal excitability focus, the AIS, was vital since genetic-based channel upregulations were linked to an increased burst firing and to absence epilepsy disorders [18, 19, 50]. Then, in order to address the main pathogenic event, we need to shed light on single-cell and local neurotransmission processes that are difficult to measure experimentally. Therefore, computational neuroscience represents one of the best solutions for understanding a problem that could help develop new potential therapeutics that avoid the common actual side effects and that treat non-responding treatment absence epilepsies. To achieve this, and as previously seen in this thesis, a compartmentalized integrate-and-fire model extended to include the AIS T-type calcium channels and fitted to experimental layer 5 primary SoCx pyramidal data was designed and developed. In addition, to gain insight into local neuronal processes, we build different SoCx networks representing different real possible local synaptic networks.

As observed in Fig. 16, the AIS T-type calcium channel fitted model allowed the neuron to fire consecutive spikes that could be action potential bursts, depending on the input and their interval spike time. The calcium channel model is demonstrated to be relatively accurate to reality as it is a transient channel, opens at relatively low voltages, and it has a considerable recovery time [17, 18, 39, 50]. Moreover, the action of the AIS T-type calcium channels implies a higher AHP response, as also seen experimentally and in Fig. 16 [57]. As detailed in the above sections, if the channel can recover sufficiently, the subsequent spike could be an action potential burst. As a result of that, and as seen in the results, it is fair to say that the AIS T-type calcium channel affects more low-input and low-frequency network environments. It makes much sense since its main pathological event happens at low frequencies, 3Hz [12, 13]. Despite this fact, as seen in clinical studies and in this thesis, an increased background (beta and gamma) EEG activity could also be seen in ictal periods resulting from increased rhythms in local synaptic SoCx networks.

Once we studied the neuronal bursting intrinsic mechanisms and see that the AIS T-type calcium channel is responsible for the short burst firing, we wanted to study its effect on different possible SoCx absence seizure networks as we previously saw that there are environments more susceptible to have a higher impact in epileptogenesis. T-type calcium channel upregulations are associated with a higher expression or performance; therefore, we model different conductance ranging from knock-out to upregulation variants.

Firstly, we model only a pyramidal excitatory network from the SoCx since GABA interneurons are the only AIS regulators, and their dysfunction has been linked to increased epileptogenesis [65, 82]. As seen in Fig. 17, the changes in the power spectrum density and, therefore, in pyramidal synchronicity appear to be the most significant among all the nets. Hence, suggesting and explaining why interneuron deficiencies combined with channel upregulations could create a potential focus for absence seizures initiation. The synchronicity augmentation correlates with bigger AIS T-type calcium conductances and

increases in single-cell pyramidal burst firing, as detailed in Fig. 18. Furthermore, the time-frequency plots in Fig. 19 also show similar synchronicity results in time. This robust result could demonstrate and explain all that has been seen in previous in vivo studies and shed light to future treatments to focus on pyramidal only or low-input nets [65, 82].

Secondly, we built a SOM-dominating network to generate beta rhythms to corroborate and see if an increase in AIS T-type calcium conductance affects different local networks. In fact, similar results have been seen in these networks. Although the relative change is not as significant as the pyramidal network, an effect on those channels also increases synchronicity through an increase in burst firing (Fig. 21). A common remark among all the network configurations, and that is pretty interesting, is that the AIS T-type calcium channel is not responsible for changing the oscillatory pattern or band; it only promotes its synchronicity. This could make us think that AIS T-type calcium channels trigger a hypersynchronous state in the SoCx, but the final trigger mechanism for the appearance of absence seizures is the disruption with the thalamus that interacts as a resonant circuit.

Thirdly, we built a PV-dominating network to generate gamma rhythms, as seen in previous experimental studies, to see if an increase in AIS T-type conductance affects local network synchronicity in this band. Surprisingly, the synchronicity increases together with the conductance, but the relative change was not as pronounced as before, indicating that the T-type calcium channel losses part of its function. This could be resulting of three different aspects: gamma frequencies are too elevated for AIS T-type calcium channels proper recovery, high inputs allow the cell to be always in more depolarized states, thus, not activating T-type currents or stochastic spike trains, with high inputs, recreate burst firing from other neurons and differences are not as noticeable. Despite this fact, an increase in bursting is also seen as well as a slight increase in synchronicity, meaning that there is a limit where burst firing increase affects synchronicity.

Finally, we built a symmetrically coupled network to see how a dynamic net with the two bands behaves. As expected, the AIS T-type calcium channel increases synchronicity in both ranges, but a higher increase was seen in low-frequencies.

All in all, we have been able to prove the thesis hypothesis as we have related upregulations in T-type calcium channels to elevated bursting behaviours and hypersynchronization states in the primary SoCx layer 5. Therefore, explaining the importance that these channels could have in triggering absence seizure epilepsy. Moreover, we have been able to demonstrate that network configuration, inputs, and oscillatory patterns play a central role in generating hypersynchrony states. As far as we are concerned, this work presents the first SoCx AIS T-type calcium channel model and the first pyramidal model to include HVA and AIS T-type calcium channel bursting mechanisms. Moreover, it is the first time that the AIS T-type role in local neurotransmission and in different networks was clearly seen.

4.1 Conclusion and Future Perspectives

To conclude this study, we can first corroborate that AIS T-type calcium channel upregulations could be triggering absence seizures. Results show that channel upregulations are linked to increased burst firing and hypersynchronization states, thus, generating a hyperexcitable focus in the SoCx for epileptogenesis. In fact, we have understood the effects of different upregulations in different possible SoCx configuration networks. Some configurations, like the low-input and low-frequencies, have been seen to be more potential epileptogenic than others. All in all, we demonstrated that an abnormal increase in the intensity of T-type calcium currents increases neurotransmission, which leads to bursting and hypersynchrony. Then, it is fair to say that we have proved our hypothesis as upregulations of the AIS T-type calcium channels were correlated with an increase in burst firing and synchronicity in local SoCx networks that could trigger absence seizures. That said, further steps are needed to be taken in order to give final insights into the absence seizure initiation mechanisms.

An example could be creating a thalamus network that interacts with the one designed in this study to see how SWD arises from a hyperexcitability focus in the SoCx. This could help in understanding how feedbacks are disrupted or how interactions are behaving during ictal periods. Furthermore, the study of the effects of T-type calcium channels in other neuronal cells from the network could be of interest to see if they have implications on synchronicity states. A final example could be studying the resulting rhythmogenesis from the interaction between local networks with T-type calcium channels and global rhythms, which could potentially explain bursting interaction and information transfer between different areas. Other pathologies need to be further studied also as they have been possibly related to this channel's dysfunction.

This thesis represents a further step into understanding absence seizure initiation by using computational neuroscience models to gain insight into behaviour and dynamics challenging to see in vivo. As absence seizure epilepsies, like childhood absence epilepsies, are severe illnesses that affect millions of people worldwide, we encourage extending the research. Projects like this could be helpful in an area where computational modelling could make a big difference.

Bibliography

[1] Christof Koch. "The End of the Beginning for the Brain". In: *Science* 339.6121 (2013), pp. 759–760. DOI: 10.1126/science.1233813.

[2] Solomon L Moshé et al. "Epilepsy: new advances". In: *The Lancet* 385.9971 (2015), pp. 884–898. DOI: 10.1016/S0140-6736(14)60456-6.

[3] Gerald W Zamponi. "Targeting voltage-gated calcium channels in neurological and psychiatric diseases". In: *Nature Reviews Drug Discovery* 15.January (2016). DOI: 10.1038/nrd.2015.5.

[4] Vincenzo Crunelli et al. "Clinical and experimental insight into pathophysiology, comorbidity and therapy of absence seizures". In: *Brain* 143.8 (May 2020), pp. 2341–2368. DOI: 10.1093/brain/awaa072.

[5] Guillaume Jarre et al. "Building up absence seizures in the somatosensory cortex: From network to cellular epileptogenic processes". In: *Cerebral Cortex* 27.9 (2017), pp. 4607–4623. DOI: 10.1093/cercor/bhx174.

[6] M. Chipaux, S. Charpier, and P. O. Polack. "Chloride-mediated inhibition of the ictogenic neurones initiating genetically-determined absence seizures". In: *Neuroscience* 192 (2011), pp. 642–651. DOI: 10.1016/j.neuroscience.2011.06.037.

[7] Pawel Glaba et al. "Changes in Interictal Pretreatment and Posttreatment EEG in Childhood Absence Epilepsy". In: *Frontiers in Neuroscience* 14 (2020), p. 196. DOI: 10.3389/fnins.2020.00196.

[8] Yucai Chen, William Davis Parker, and Keling Wang. "The Role of T-Type Calcium Channel Genes in Absence Seizures". In: *Frontiers in Neurology* 5 (2014), p. 45. DOI: 10.3389/fneur.2014.00045.

[9] Carl E. Stafstrom and Lionel Carmant. "Seizures and Epilepsy: An Overview for Neuroscientists". In: *Cold Spring Harb Perspect Med* 5.6 (2015). DOI: 10.1101/cshperspect.a022426.

[10] Massimo Avoli. "A brief history on the oscillating roles of thalamus and cortex in absence seizures". In: *Epilepsia* 53.5 (2012), pp. 779–789. DOI: 10.1111/j.1528-1167.2012.03421.x.

[11] J. P.A. Manning et al. "Cortical-area specific block of genetically determined absence seizures by ethosuximide". In: *Neuroscience* 123.1 (2004), pp. 5–9. DOI: 10.1016/j.neuroscience.2003.09.026.

[12] Annika Lüttjohann and Hans Christian Pape. "Regional specificity of cortico-thalamic coupling strength and directionality during waxing and waning of spike and wave discharges". In: *Scientific Reports* 9.1 (2019). DOI: 10.1038/s41598-018-37985-7.

[13] Krisztina Benedek et al. "Neocortical gamma oscillations in idiopathic generalized epilepsy". In: *Epilepsia* 57.5 (2016), pp. 796–804. DOI: 10.1111/epi.13355.

[14] Pierre Olivier Polack et al. "Deep layer somatosensory cortical neurons initiate spike-and-wave discharges in a genetic model of absence seizures". In: *Journal of Neuroscience* 27.24 (2007), pp. 6590–6599. DOI: 10.1523/JNEUROSCI.0753-07.2007.

[15] Antoine Depaulis, Olivier David, and Stéphane Charpier. "The genetic absence epilepsy rat from Strasbourg as a model to decipher the neuronal and network mechanisms of generalized idiopathic epilepsies". In: *Journal of Neuroscience Methods* 260 (2016), pp. 159–174. DOI: 10.1016/j.jneumeth.2015.05.022.

[16] Ghazaleh Ghamkhari Nejad et al. "Ethosuximide affects paired-pulse facilitation in somatosensory cortex of WAGrats as a model of absence seizure". In: *Advanced Pharmaceutical Bulletin* 5.4 (2015), pp. 483–489. DOI: 10.15171/apb.2015.066.

[17] Stuart M. Cain and Terrance P. Snutch. "T-type calcium channels in burst-firing, network synchrony, and epilepsy". In: *Biochimica et Biophysica Acta - Biomembranes* 1828.7 (2013), pp. 1572–1578. DOI: 10.1016/j.bbamem.2012.07.028.

[18] Yucai Chen et al. "Association between genetic variation of CACNA1H and childhood absence epilepsy". In: *Annals of Neurology* 54.2 (2003), pp. 239–243. DOI: 10.1002/ana.10607.

[19] Verena C. Wimmer et al. "Axon initial segment dysfunction in epilepsy". In: *Journal of Physiology* 588.11 (2010), pp. 1829–1840. ISSN: 00223751. DOI: 10.1113/jphysiol.2010.188417.

[20] Houman Khosravani et al. "Effects of Cav3.2 channel mutations linked to idiopathic generalized epilepsy". In: *Annals of Neurology* 57.5 (2005), pp. 745–749. DOI: 10.1002/ana.20458.

[21] Stuart M. Cain and Terrance P. Snutch. "Contributions of T-type calcium channel isoforms to neuronal firing". In: *Channels* 4.6 (2010), pp. 475–482. DOI: 10.4161/chan.4.6.14106.

[22] Kim L. Powell et al. "A Cav3.2 T-type calcium channel point mutation has splice-variant-specific effects on function and segregates with seizure expression in a polygenic rat model of absence epilepsy". In: *Journal of Neuroscience* 29.2 (2009), pp. 371–380. DOI: 10.1523/JNEUROSCI.5295-08.2009.

[23] Karen M. J. van Loo and Albert J. Becker. "Transcriptional Regulation of Channelopathies in Genetic and Acquired Epilepsies". In: *Frontiers in Cellular Neuroscience* 13 (2020), p. 587. DOI: 10.3389/fncel.2019.00587.

[24] Norbert Weiss and Gerald W. Zamponi. "Genetic T-type calcium channelopathies". In: *Journal of Medical Genetics* 57.1 (2020), pp. 1–10. DOI: 10.1136/jmedgenet-2019-106163.

[25] Henrik Alle and Jörg R.P. Geiger. "Combined analog and action potential coding in hippocampal mossy fibers". In: *Science* 311.5765 (2006), pp. 1290–1293. DOI: 10.1126/science.1119055.

[26] Bruce P. Bean. "The action potential in mammalian central neurons". In: *Nature Reviews Neuroscience* 8.6 (2007), pp. 451–465. DOI: 10.1038/nrn2148.

[27] Kenneth D. Harris et al. "Temporal interaction between single spikes and complex spike bursts in hippocampal pyramidal cells". In: *Neuron* 32.1 (2001), pp. 141–149. DOI: 10.1016/S0896-6273(01)00447-0.

[28] Rüdiger Krahe and Fabrizio Gabbiani. "Burst firing in sensory systems". In: *Nature Reviews Neuroscience* 5.1 (2004), pp. 13–23. DOI: 10.1038/nrn1296.

[29] Lucy M. Palmer and Greg J. Stuart. "Site of action potential initiation in layer 5 pyramidal neurons". In: *Journal of Neuroscience* 26.6 (2006), pp. 1854–1863. DOI: 10.1523/JNEUROSCI.4812-05.2006.

[30] Costa M. Colbert and Daniel Johnston. "Axonal action-potential initiation and Na+ channel densities in the soma and axon initial segment of subicular pyramidal neurons". In: *Journal of Neuroscience* 16.21 (1996), pp. 6676–6686. DOI: 10.1523/jneurosci.16-21-06676.1996.

[31] J. S. Coombs, D. R. Curtis, and J. C. Eccles. "The interpretation of spike potentials of motoneurones." In: *The Journal of Physiology* 139.2 (1957), pp. 198–231. DOI: 10.1113/jphysiol.1957.sp005887.

[32] Matthew S. Grubb and Juan Burrone. "Activity-dependent relocation of the axon initial segment fine-tunes neuronal excitability". In: *Nature* 465.7301 (2010), pp. 1070–1074. DOI: 10.1038/nature09160.

[33] Maarten H.P. Kole and Greg J. Stuart. "Signal Processing in the Axon Initial Segment". In: *Neuron* 73.2 (2012), pp. 235–247.

[34] Claire Yu Mei Huang and Matthew N. Rasband. "Axon initial segments: structure, function, and disease". In: *Annals of the New York Academy of Sciences* 1420.1 (2018), pp. 46–61. DOI: 10.1111/nyas.13718.

[35] Shelly A. Buffington and Matthew N. Rasband. "The axon initial segment in nervous system disease and injury". In: *European Journal of Neuroscience* 34.10 (2011), pp. 1609–1619. DOI: 10.1111/j.1460-9568.2011.07875.x.

[36] Maarten H.P. Kole et al. "Action potential generation requires a high sodium channel density in the axon initial segment". In: *Nature Neuroscience* 11.2 (2008), pp. 178–186. DOI: 10.1038/nn2040.

[37] Andrea Lorincz and Zoltan Nusser. "Cell-type-dependent molecular composition of the axon initial segment". In: *Journal of Neuroscience* 28.53 (2008), pp. 14329–14340. DOI: 10.1523/JNEUROSCI.4833-08.2008.

[38] W H Moolenaar and I Spector. "Ionic currents in cultured mouse neuroblastoma cells under voltage-clamp conditions." In: *The Journal of Physiology* 278.1 (1978), pp. 265–286. DOI: https://doi.org/10.1113/jphysiol.1978.sp012303.

[39] Edward Perez-Reyes. "Molecular physiology of low-voltage-activated T-type calcium channels". In: *Physiological Reviews* 83.1 (2003), pp. 117–161. DOI: 10.1152/physrev.00018.2002.

[40] G. Callewaert, J. Eilers, and A. Konnerth. "Axonal calcium entry during fast 'sodium' action potentials in rat cerebellar Purkinje neurones". In: *Journal of Physiology* 495.3 (1996), pp. 641–647. DOI: 10.1113/jphysiol.1996.sp021622.

[41] Marc Chevalier et al. "T-type Cav3.3 calcium channels produce spontaneous low-threshold action potentials and intracellular calcium oscillations". In: *European Journal of Neuroscience* 23.9 (2006), pp. 2321–2329. DOI: 10.1111/j.1460-9568.2006.04761.x.

[42] Norbert Weiss and Gerald W. Zamponi. "T-type calcium channels: From molecule to therapeutic opportunities". In: *International Journal of Biochemistry and Cell Biology* 108 (2019), pp. 34–39. DOI: 10.1016/j.biocel.2019.01.008.

[43] Philippe Lory, Sophie Nicole, and Arnaud Monteil. "Neuronal Cav3 channelopathies: recent progress and perspectives". In: *Pflugers Archiv European Journal of Physiology* 472.7 (2020), pp. 831–844. DOI: 10.1007/s00424-020-02429-7.

[44] John R. Huguenard. "Low-voltage-activated (T-type) calcium-channel genes identified". In: *Trends in Neurosciences* 21.11 (1998), pp. 451–452. DOI: 10.1016/S0166-2236(98)01331-9.

[45] Guangfu Wang et al. "Cav3.2 calcium channels control NMDA receptor-mediated transmission: A new mechanism for absence epilepsy". In: *Genes and Development* 29.14 (2015), pp. 1535–1551. DOI: 10.1101/gad.260869.115.

[46] Brett A. Simms and Gerald W. Zamponi. "Neuronal voltage-gated calcium channels: Structure, function, and dysfunction". In: *Neuron* 82.1 (2014), pp. 24–45. DOI: 10.1016/j.neuron.2014.03.016.

[47] Bruce E. McKay et al. "CaV3 T-type calcium channel isoforms differentially distribute to somatic and dendritic compartments in rat central neurons". In: *European Journal of Neuroscience* 24.9 (2006), pp. 2581–2594. DOI: 10.1111/j.1460-9568.2006.05136.x.

[48] Carolina Aguado et al. "Ontogenic changes and differential localization of T-type Ca2+ channel subunits Cav3.1 and Cav3.2 in mouse hippocampus and cerebellum". In: *Frontiers in Neuroanatomy* 10 (2016), p. 83. DOI: 10.3389/fnana.2016.00083.

[49] Benjamin J. Kopecky, Ruqiang Liang, and Jianxin Bao. "T-type calcium channel blockers as neuroprotective agents". In: *Pflugers Archiv European Journal of Physiology* 466.4 (2014), pp. 757–765. DOI: 10.1007/s00424-014-1454-x.

[50] Stuart M. Cain and Terrance P. Snutch. "Contributions of T-type calcium channel isoforms to neuronal firing". In: *Channels* 4.6 (2010), pp. 475–482. DOI: 10.4161/chan.4.6.14106.

[51] Jin Yong Park et al. "Multiple structural elements contribute to the slow kinetics of the Ca v3.3 T-type channel". In: *Journal of Biological Chemistry* 279.21 (2004), pp. 21707–21713. DOI: 10.1074/jbc.M400684200.

[52] Kevin J. Bender and Laurence O. Trussell. "Axon Initial Segment Ca2+ Channels Influence Action Potential Generation and Timing". In: *Neuron* 61.2 (2009), pp. 259–271. DOI: 10.1016/j.neuron.2008.12.004.

[53] Kevin J. Bender, Christopher P. Ford, and Laurence O. Trussell. "Dopaminergic Modulation of Axon Initial Segment Calcium Channels Regulates Action Potential Initiation". In: *Neuron* 68.3 (2010), pp. 500–511. DOI: 10.1016/j.neuron.2010.09.026.

[54] Kevin J. Bender et al. "Control of firing patterns through modulation of axon initial segment T-type calcium channels". In: *Journal of Physiology* 590.1 (2012), pp. 109–118. DOI: 10.1113/jphysiol.2011.218768.

[55] Casey R. Vickstrom et al. "T-type calcium channels contribute to burst firing in a subpopulation of medial habenula neurons". In: *eNeuro* 7.4 (2020). DOI: 10.1523/ENEURO.0201-20.2020.

[56] Daesoo Kim et al. "Lack of the burst firing of thalamocortical relay neurons and resistance to absence seizures in mice lacking α1G T-type Ca2+ channels". In: *Neuron* 31.1 (2001), pp. 35–45. DOI: 10.1016/S0896-6273(01)00343-9.

[57] Miriam Candelas et al. "Cav3.2 T-type calcium channels shape electrical firing in mouse Lamina II neurons". In: *Scientific Reports* 9 (2019). DOI: 10.1038/s41598-019-39703-3.

[58] Ya Chin Yang et al. "The T-type calcium channel as a new therapeutic target for Parkinson's disease". In: *Pflugers Archiv European Journal of Physiology* 466.4 (2014), pp. 747–755. DOI: 10.1007/s00424-014-1466-6.

[59] Jordi Garcia-Ojalvo and Jose Sancho. *Noise in Spatially Extended Systems*. Institute for Nonlinear Science. Springer-Verlag New York, 1999. ISBN: 978-1-4612-1536-3. DOI: 10.1007/978-1-4612-1536-3.

[60] Henry C. Tuckwell. *Introduction to Theoretical Neurobiology*. Vol. 2. Cambridge Studies in Mathematical Biology. Cambridge University Press, 1988. DOI: 10.1017/CBO9780511623271.

[61] A Destexhe et al. "Fluctuating synaptic conductances recreate in vivo-like activity in neocortical neurons". In: *Neuroscience* 107.1 (2001), pp. 13–24. DOI: 10.1016/S0306-4522(01)00344-X.

[62] Matthew E. Larkum, Walter Senn, and Hans R. Lüscher. "Top-down dendritic input increases the gain of layer 5 pyramidal neurons". In: *Cerebral Cortex* 14.10 (2004), pp. 1059–1070. DOI: 10.1093/cercor/bhh065.

[63] Peter Dayan and L. F. Abbott. *Theoretical Neuroscience: Computational and Mathematical Modeling of Neural Systems*. The MIT Press, 2005. ISBN: 0262541858. DOI: 10.5555/1205781.

[64] Nelson Spruston. "Pyramidal neurons: Dendritic structure and synaptic integration". In: *Nature Reviews Neuroscience* 9 (2008), pp. 206–221. DOI: 10.1038/nrn2286.

[65] John M. Bekkers. "Pyramidal neurons". In: *Current Biology* 21.24 (2011), R975. DOI: 10.1016/j.cub.2011.10.037.

[66] Alessandra Donato et al. "Neuronal sub-compartmentalization: a strategy to optimize neuronal function". In: *Biological Reviews* 94.3 (2019), pp. 1023–1037. DOI: 10.1111/brv.12487.

[67] Nace L. Golding et al. "Dendritic calcium spike initiation and repolarization are controlled by distinct potassium channel subtypes in CA1 pyramidal neurons". In: *Journal of Neuroscience* 19.20 (1999), pp. 8789–8798. DOI: 10.1523/jneurosci.19-20-08789.1999.

[68] Björn M. Kampa and Greg J. Stuart. "Calcium spikes in basal dendrites of layer 5 pyramidal neurons during action potential bursts". In: *Journal of Neuroscience* 26.28 (2006), pp. 7424–7432. DOI: 10.1523/JNEUROSCI.3062-05.2006.

[69] Henry Alitto et al. "The Augmentation of Retinogeniculate Communication during Thalamic Burst Mode". In: *Journal of Neuroscience* 39.29 (2019), pp. 5697–5710. DOI: 10.1523/JNEUROSCI.2320-18.2019.

[70] J. R. Huguenard and D. A. McCormick. "Simulation of the currents involved in rhythmic oscillations in thalamic relay neurons". In: *Journal of Neurophysiology* 68.4 (1992), pp. 1373–1383. DOI: 10.1152/jn.1992.68.4.1373.

[71] J. R. Huguenard and D. A. Prince. "A novel T-type current underlies prolonged Ca2+-dependent burst firing in GABAergic neurons of rat thalamic reticular nucleus". In: *Journal of Neuroscience* 12.10 (1992), pp. 3804–3817. DOI: 10.1523/jneurosci.12-10-03804.1992.

[72] Kamal Abu-Hassan et al. "Optimal solid state neurons". In: *Nature Communications* 10.1 (2019). DOI: 10.1038/s41467-019-13177-3.

[73] Charlotte Deleuze et al. "T-type calcium channels consolidate tonic action potential output of thalamic neurons to neocortex". In: *Journal of Neuroscience* 32.35 (2012), pp. 12228–12236. DOI: 10.1523/JNEUROSCI.1362-12.2012.

[74] Sébastien Béhuret et al. "Cortically-Controlled Population Stochastic Facilitation as a Plausible Substrate for Guiding Sensory Transfer across the Thalamic Gateway". In: *PLoS Computational Biology* 9.12 (2013). DOI: 10.1371/journal.pcbi.1003401.

[75] Haiyang Wei et al. "Thalamic burst firing propensity: A comparison of the dorsal lateral geniculate and pulvinar nuclei in the tree shrew". In: *Journal of Neuroscience* 31.47 (2011), pp. 17287–17299. DOI: 10.1523/JNEUROSCI.6431-10.2011.

[76] E. Carbone and H. D. Lux. "A low voltage-activated, fully inactivating Ca channel in vertebrate sensory neurones". In: *Nature* 310 (1984), pp. 501–502. DOI: 10.1038/310501a0.

[77] Nathalie Leresche and Régis C. Lambert. "T-type calcium channels in synaptic plasticity". In: *Channels* 11.2 (2017), pp. 121–139. DOI: 10.1080/19336950.2016.1238992.

[78] Jean Chemin et al. "Specific contribution of human T-type calcium channel isotypes (α1G, α1H and α1I) to neuronal excitability". In: *Journal of Physiology* 540.1 (2002), pp. 3–14. DOI: 10.1113/jphysiol.2001.013269.

[79] A. L. Hodgkin and A. F. Huxley. "A quantitative description of membrane current and its application to conduction and excitation in nerve". In: *The Journal of Physiology* 117.4 (1952), pp. 500–544. DOI: 10.1113/jphysiol.1952.sp004764.

[80] Toshinobu Kuki et al. "Contribution of parvalbumin and somatostatin-expressing GABAergic neurons to slow oscillations and the balance in beta-gamma oscillations across cortical layers". In: *Frontiers in Neural Circuits* 9 (2015), p. 6. DOI: 10.3389/fncir.2015.00006.

[81] Alexander Naka and Hillel Adesnik. "Inhibitory Circuits in Cortical Layer 5". In: *Frontiers in Neural Circuits* 10 (2016), p. 35. DOI: 10.3389/fncir.2016.00035.

[82] Robin Tremblay, Soohyun Lee, and Bernardo Rudy. "GABAergic Interneurons in the Neocortex: From Cellular Properties to Circuits". In: *Neuron* 91.2 (2016), pp. 260–292. DOI: 10.1016/j.neuron.2016.06.033.

[83] Jessica A. Cardin. "Inhibitory Interneurons Regulate Temporal Precision and Correlations in Cortical Circuits". In: *Trends in Neurosciences* 41.10 (2018), pp. 689–700. DOI: 10.1016/j.tins.2018.07.015. URL: https://doi.org/10.1016/j.tins.2018.07.015.

[84] Ling Liu et al. "Cell type-differential modulation of prefrontal cortical GABAergic interneurons on low gamma rhythm and social interaction". In: *Science Advances* 6.30 (2020). DOI: 10.1126/sciadv.aay4073.

[85] Eugene M. Izhikevich. *Dynamical Systems in Neuroscience The Geometry of Excitability and Bursting*. Computational Neuroscience Series. The MIT Press, 2006. ISBN: 9780262090438. DOI: 10.7551/mitpress/2526.001.0001.

[86] Peter McColgan et al. "The human motor cortex microcircuit: insights for neurodegenerative disease". In: *Nature Reviews Neuroscience* 21 (2020), pp. 401–415. DOI: 10.1038/s41583-020-0315-1.

[87] Guang Chen et al. "Distinct Inhibitory Circuits Orchestrate Cortical beta and gamma Band Oscillations". In: *Neuron* 96.6 (2017), 1403–1418.e6. DOI: 10.1016/j.neuron.2017.11.033.

[88] Srikanth Ramaswamy and Henry Markram. "Anatomy and physiology of the thick-tufted layer 5 pyramidal neuron". In: *Frontiers in Cellular Neuroscience* 9 (2015), p. 233. DOI: 10.3389/fncel.2015.00233.

[89] Jaime E. Heiss et al. "Shift in the balance between excitation and inhibition during sensory adaptation of S1 neurons". In: *Journal of Neuroscience* 28.49 (2008), pp. 13320–13330. DOI: 10.1523/JNEUROSCI.2646-08.2008.

[90] Michael J. Higley and Diego Contreras. "Balanced excitation and inhibition determine spike timing during frequency adaptation". In: *Journal of Neuroscience* 26.2 (2006), pp. 448–457. DOI: 10.1523/JNEUROSCI.3506-05.2006.

[91] Maxwell A. Sherman et al. "Neural mechanisms of transient neocortical beta rhythms: Converging evidence from humans, computational modeling, monkeys, and mice". In: *Proceedings of the National Academy of Sciences of the United States of America* 113.33 (2016), E4885–E4894. DOI: 10.1073/pnas.1604135113.

[92] Anne M.M. Fransen et al. "Distinct α- and β-band rhythms over rat somatosensory cortex with similar properties as in humans". In: *Journal of Neurophysiology* 115.6 (2016), pp. 3030–3044. DOI: 10.1152/jn.00507.2015.

[93] O. Jensen et al. "On the human sensorimotor-cortex beta rhythm: Sources and modeling". In: *NeuroImage* 26.2 (2005), pp. 347–355. DOI: 10.1016/j.neuroimage.2005.02.008.

[94] Linette Liqi Tan et al. "Gamma oscillations in somatosensory cortex recruit prefrontal and descending serotonergic pathways in aversion and nociception". In: *Nature Communications* 10.1 (2019). DOI: 10.1038/s41467-019-08873-z.

[95] Weiguo Yang and Qian Quan Sun. "Circuit-specific and neuronal subcellular-wide E-I balance in cortical pyramidal cells". In: *Scientific Reports* 8 (2018). DOI: 10.1038/s41598-018-22314-9.

[96] Loreen Hertäg and Henning Sprekeler. "Amplifying the redistribution of somatodendritic inhibition by the interplay of three interneuron types". In: *PLoS Computational Biology* 15.5 (2019). DOI: 10.1371/journal.pcbi.1006999.

[97] Thilo Womelsdorf et al. "Burst firing synchronizes prefrontal and anterior cingulate cortex during attentional control". In: *Current Biology* 24.22 (2014), pp. 2613–2621. DOI: 10.1016/j.cub.2014.09.046.

[98] D.J. Thomson. "Spectrum estimation and harmonic analysis". In: *Proceedings of the IEEE* 70.9 (1982), pp. 1055–1096. DOI: 10.1109/PROC.1982.12433.

[99] Mike X Cohen. *Analyzing Neural Time Series Data: Theory and Practice*. The MIT Press, 2014. ISBN: 9780262019873. DOI: 10.7551/mitpress/9609.001.0001.

[100] Mael Dumenieu et al. “The low-threshold calcium channel Cav3.2 mediates burst firing of mature dentate granule cells”. In: *Cerebral Cortex* 28.7 (2018), pp. 2594–2609. DOI: 10.1093/cercor/bhy084.

[101] Constance Hammond. *Cellular and Molecular Neurophysiology: Fourth Edition*. Fourth Edition. Elsevier Ltd, 2015. ISBN: 9780123970329. DOI: 10.1016/B978-0-12-397032-9.00003-0.

Supplementary information

S.I Ornstein-Uhlenbeck Derivation by Itô's Calculus

To obtain the Ornstein-Uhlenbeck formula used in the models (See Section 2.1.1) we must derived it from its Langevin form. The resulting equation is similar to the one used by Larkum and co-workers and will enable us to integrate it using a Forward Euler Method to model a stochastic injected neuronal inputs that depend on the previous state [62].

For that, firstly, we must consider that an Ornstein-Uhlenbeck stochastic process can be described by the following stochastic differential equation (Described by Destexhe and co-workers to reproduce in vivo-like neuronal inputs) [61]:

$$\frac{dX_t}{dt} = \lambda(\mu - X_t) + \sqrt{D}\,\frac{dW_t}{dt} \tag{S.1}$$

The parameter μ stands for the process mean, D for the stochastic process amplitude, and λ for the inverse correlation time. dW_t/dt is the differential of a Wiener process. To solve this problem, we pass dt to the other side:

$$dX_t = \lambda(\mu - X_t)dt + \sqrt{D}\,dW_t \tag{S.2}$$

Now we apply some algebra:

$$dX_t + \lambda X_t dt = \lambda\mu dt + \sqrt{D}\,dW_t \tag{S.3}$$

We multiply by the integrator factor $e^{\lambda t}$ to be able to integrate the stochastic differential equation:

$$e^{\lambda t}dX_t + e^{\lambda t}\lambda X_t dt = \lambda\mu e^{\lambda t}dt + \sqrt{D}\,e^{\lambda t}\,dW_t \tag{S.4}$$

By applying Itô's calculus product rule ($d(X_tY_t) = X_tdY_t + Y_tdX_t + dX_tdY_t$) with a cross-term equal to 0 (Because in our case Y_t is non-stochastic) we get that:

$$d(e^{\lambda t}X_t) = \lambda\mu e^{\lambda t}dt + \sqrt{D}\,e^{\lambda t}dW_t \tag{S.5}$$

We integrate for $[t, t+dt]$:

$$\int_t^{t+dt} d(e^{\lambda t}X_t) = \int_t^{t+dt} \lambda\mu e^{\lambda t}dt + \sqrt{D}\int_t^{t+dt} e^{\lambda t}dW_t \tag{S.6}$$

If we integrate:

$$e^{\lambda(t+dt)}X_{t+dt} - e^{\lambda t}X_t = \mu(e^{\lambda(t+dt)} - e^{\lambda t}) + \sqrt{D}\int_t^{t+dt} e^{\lambda t}dW_t \tag{S.7}$$

We multiply everything by $e^{-\lambda(t+dt)}$ and isolate:

$$X_{t+dt} = X_t e^{-\lambda dt} + \mu(1 - e^{-\lambda dt}) + \sqrt{D}\int_t^{t+dt} e^{-\lambda dt}dW_t \tag{S.8}$$

Applying Itô's isometry rule, we know that:

$$E[X_{t+dt}] = X_t e^{-\lambda dt} + \mu(1 - e^{-\lambda dt}) \tag{S.9}$$

$$V[X_{t+dt}] = \frac{D}{2\lambda}(1 - e^{-2\lambda dt}) \tag{S.10}$$

Therefore, knowing that Itô's integral of a deterministic integrand is normally distributed, we can rewrite:

$$X_{t+dt} = X_t e^{-\lambda dt} + \mu(1 - e^{-\lambda dt}) + N[0,1]\sqrt{D}\sqrt{\frac{1 - e^{-2\lambda dt}}{2}} \tag{S.11}$$

As dt corresponds to 0.0001 seconds in our simulations we can apply the approximation $e^x \approx 1 + x$. Then, by applying some algebra and the conversions, $\sigma^2 = \frac{D\tau}{2}$ (Due to x being a gaussian process) and $\lambda = \frac{1}{\tau}$, we get the final equation used in Section 2.1.1:

$$X_{t+dt} = X_t + \frac{\mu - X_t}{\tau}dt + \sigma N[0,1]\sqrt{\frac{2dt}{\tau}} \tag{S.12}$$

S.II Model Parameters

S.II.1 Layer 5 Somatosensory Cortex Pyramidal Model

These are the parameters extracted from Larkum et al. (2004) and used to model the two compartmentalized integrate-and-fire Layer 5 SoCx pyramidal neuron model that has been used in the thesis [62].

Parameter	Symbol	Value	Unit
Dendrite resting membrane potential	$V_{rest,D}$	-60	mV
Somatic resting membrane potential	$V_{rest,S}$	-70	mV
Dendrite total membrane capacitance	C_D	120	pF
Somatic total membrane capacitance	C_S	260	pF
Dendrite total membrane resistance	R_D	43	$M\Omega$
Somatic total membrane resistance	R_S	50	$M\Omega$
Transfer coupling resistance	R_T	65	$M\Omega$
Maximal HVA conductance	g_{HVA}	70	nS
Maximal AHP conductance	g_{AHP}	4	nS
Potassium reversal potential	E_K	-90	mV
AHP decay time constant	τ_k	80	ms
HVA activation gate decay time constant	τ_m	80	ms
HVA inactivation gate decay time	τ_h	15	ms
HVA activation gate slope	S_m	$-1/2$	mV^{-1}
HVA inactivation gate slope	S_h	$1/2$	mV^{-1}
HVA activation half-activation	$m_{1/2}$	-9	mV
HVA inactivation half-activation	$h_{1/2}$	-21	mV
Threshold	Θ	-47	mV

Table S1: Layer 5 somatosensory cortex pyramidal model parameters. The parameters are extracted from Larkum et al. (2004) [62].

S.II.2 The AIS T-type Calcium Channel Model

All parameters used for the AIS T-type calcium channel model can be found in Table S2. They were mainly extracted from Chemin et al. (2002), as it shows similar results to other experimental studies and it represents Cav3.2, the most related T-type calcium channel to absence seizure [78].

Parameter	Symbol	Value	Unit	References
Calcium reversal potential	E_{Ca}	120	mV	[101]
AIS T-type activation half-activation	$m_{1/2}$	-48.4	mV	[78]
AIS T-type inactivation half-activation	$h_{1/2}$	-75.6	mV	[78]
AIS T-type activation gate slope	k_m	-5.2	mV	[78]
AIS T-type inactivation gate slope	k_h	6.2	mV	[78]
AIS T-type maximal recovery time	τ_{rec}	400	ms	[39, 78]

Table S2: AIS T-type calcium channel parameters used for simulating the channel.

S.III Additional Results

Simulations were performed using different Ornstein-Uhlenbeck injected inputs to the various networks with a μ ranging from 100 pA to 1000 pA in the pyramidal compartments. In this additional results section, we add some different results ranging from different regimes for comparison purposes. Consider that due to similar results, only some graphs are shown here.

S.III.1 SOM-dominating Network

Here, in Fig. S1 it can be seen different multitaper power spectrums for different input SOM-dominating networks. Both corresponds to an injected Ornstein-Uhlenbeck with $\mu = 100$ pA and $\mu = 750$ pA, in both compartments, respectively. Results show that upregulations in the AIS T-type calcium channels increase synchronicity, especially in low-input networks. Moreover, an increase in burst firing was correlated to this phenomenon.

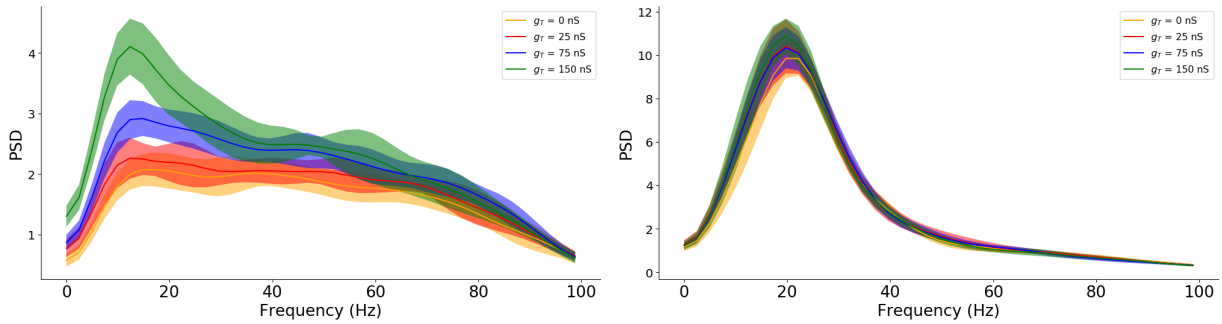

(a) **(b)**

Figure S1: SOM-dominating network multitaper power spectrum for different injected currents and AIS T-type calcium conductances. As observed, elevated T-type calcium channel conductances increase the oscillatory signal power. (a) Multitaper power spectrum range and mean for 10 simulations with an Ornstein-Uhlenbeck injection with $\mu = 100$ pA. (b) Multitaper power spectrum range and mean for 10 simulations with an Ornstein-Uhlenbeck injection with $\mu = 750$ pA.

S.III.2 PV-dominating Network

In Fig. S2, it can be observed the multitaper power spectrum for the PV-dominating network for an injected Ornstein-Uhlenbeck with $\mu = 1000$ pA in both compartments. Results show that upregulations in the AIS T-type calcium channels increase synchronicity in the PV network. Despite this fact, little change is seen as there is a high-input injection; thus, neurons do not consider much the network behaviour.

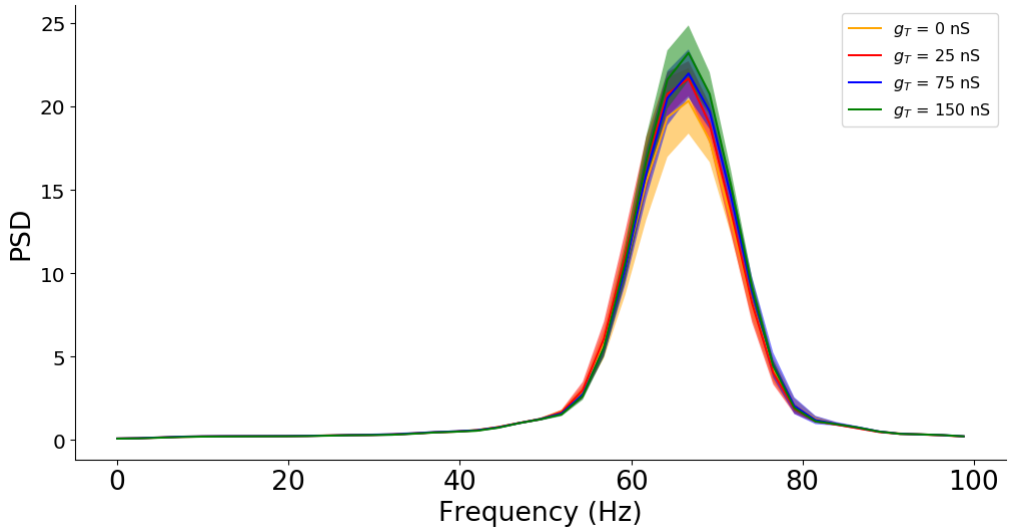

Figure S2: PV-dominating network multitaper power spectrum for different AIS T-type calcium conductances with an Ornstein-Uhlenbeck injection with $\mu = 1000$ pA. As observed, elevated T-type calcium channel conductances increase the gamma oscillatory signal power and its synchronicity.

S.III.3 Symmetrically Coupled Network

In Fig. S3, it can be seen the multitaper power spectrum for the symmetrically coupled network for an injected Ornstein-Uhlenbeck with $\mu = 250$ pA in both compartments. Results show that upregulations in the AIS T-type calcium channel lead to an increase in synchronicity in the network, but gamma frequency bands do not appear due to the low input applied.

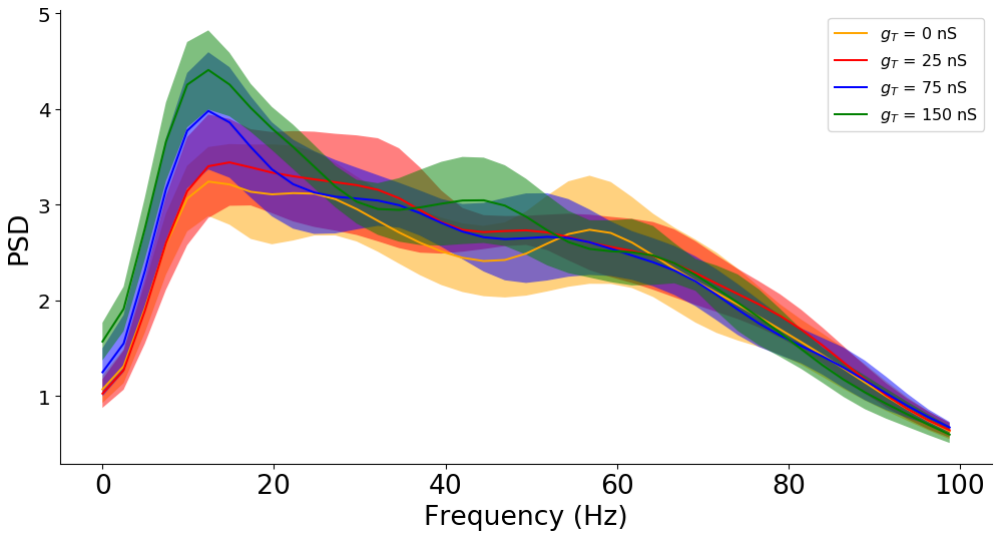

Figure S3: Symmetrically coupled network multitaper power spectrum for different AIS T-type calcium conductances with an Ornstein-Uhlenbeck injection of $\mu = 250$ pA. As observed, elevated T-type calcium channel conductances increase the oscillatory signal power and synchronicity, but gamma frequencies are not present.

Moreover, in Fig. S4 and Fig. S5 we can appreciated the burst events per simulations in single pyramidal cells and time-frequency plots, respectively, for an Ornstein-Uhlenbeck injection with $\mu = 750$ pA.

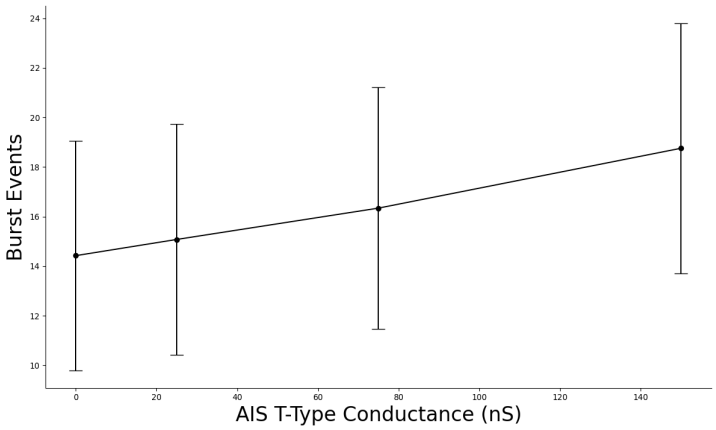

Figure S4: Symmetrically coupled network burst events per simulation for different AIS T-type calcium conductances. As observed, elevated T-type calcium channel conductances increase bursting events in pyramidal cells. Each point in the plot is an average of 8000 pyramidal cells. Error bars were represented as the mean ± the standard deviation.

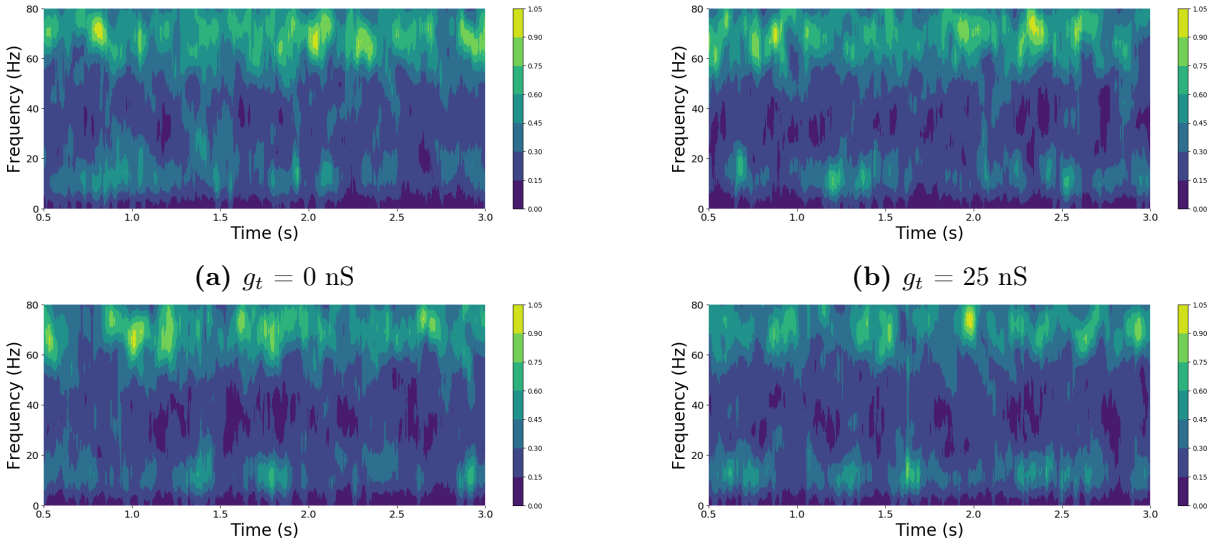

(a) $g_t = 0$ nS

(b) $g_t = 25$ nS

(c) $g_t = 75$ nS

(d) $g_t = 150$ nS

Figure S5: Symmetrically coupled network time-frequency plots for different AIS T-type calcium conductances.